SYNTHESIS AND PERFORMANCE OF BIO-BASED ANTISCALANT DERIVED FROM POLY(ITACONIC ACID)

BY

CHAKRIYA KONG

A THESIS SUBMITTED IN PARTIAL FULFILLMENT OF THE REQUIREMENTS FOR THE DEGREE OF MASTER OF ENGINEERING (ENGINEERING TECHNOLOGY)
SIRINDHORN INTERNATIONAL INSTITUTE OF TECHNOLOGY
THAMMASAT UNIVERSITY
ACADEMIC YEAR 2022

THAMMASAT UNIVERSITY
SIRINDHORN INTERNATIONAL INSTITUTE OF TECHNOLOGY

THESIS

BY

CHAKRIYA KONG

ENTITLED

SYNTHESIS AND PERFORMANCE OF BIO-BASED ANTISCALANT DERIVED FROM POLY(ITACONIC ACID)

was approved as partial fulfillment of the requirements for
the degree of Master of Engineering (Engineering Technology)

on July 11, 2023

Chairperson	(Assistant Professor Chariya Kaewsaneha, Ph.D.)
Member and Advisor	(Associate Professor Pakorn Opaprakasit, Ph.D.)
Member and Co-advisor	(Atitsa Petchsuk, Ph.D.)
Member	(Professor Ikuyoshi Tomita, Ph.D.)
Director	(Professor Pruettha Nanakorn, D.Eng.)

Thesis Title	SYNTHESIS AND PERFORMANCE OF BIO-BASED ANTISCALANT DERIVED FROM POLY(ITACONIC ACID)
Author	Chakriya Kong
Degree	Master of Engineering (Engineering Technology)
Faculty/University	Sirindhorn International Institute of Technology/ Thammasat University
Thesis Advisor	Associate Professor Pakorn Opaprakasit, Ph.D.
Thesis Co-Advisor	Atitsa Petchsuk, Ph.D.
Academic Years	2022

ABSTRACT

Scale formation in water-treatment facilities is a critical issue due to serious reductions in the unit's performance and possible damage to the system. An addition of antiscalants is essential in coping with this problem. However, the majority of these are non-degradable and derived from non-renewable resources, which may cause serious concerns to the environment. Itaconic acid (IA) is an unsaturated dicarboxylic acid produced by biomass fermentation. The material is non-toxic, renewable, and biodegradable. In this work, a process for synthesizing poly(itaconic acid) (PIA) as a bio-based antiscalant is developed. PIA was synthesized by three different methods, i.e., emulsion polymerization, phase inversion emulsification, and free radical polymerization. A suitable method for synthesizing PIA was selected to optimize the effects of pH of IA and initiator concentration on the PIA structure and performance. The chemical structures of the resulting polymer are then characterized by Fourier transforms infrared (FTIR) and proton nuclear magnetic resonance (^{1}H-NMR) spectroscopy and gel permeation chromatography (GPC). The inhibition efficiency against a calcium carbonate scale of the synthesized materials is assessed by using inductively coupled plasma-optical emission spectroscopy (ICP-OES). An effective material was selected to investigate their scale inhibition performance. The inhibition

mechanism of PIA against calcium carbonate ($CaCO_3$) was investigated. The results show that free radical polymerization is a potential method for synthesizing PIA, at an optimum polymerization time of 4 h at 85 ℃. The variation of pH of IA before polymerization indicated that neutralizing IA to pH 4 enhances the free radical stability and improves the monomer conversion rate to 100 %, while neutralizing IA at pH 9 causes ion repulsion and reduces the monomer conversion rate to 75%. In addition, neutralizing IA to higher pH boosted the deprotonation of COOH, leading to excellent inhibition performance. Increasing the initiator concentration from 5 to 14% improved monomer conversion from 61 to 96%, respectively, due to the generation of free radicals. The reduction of molecular weight based on the initiator dosage is caused by a high possibility of the termination stage during free radical polymerization. However, molecular weight has a potential impact on inhibition efficiency. High molecular weight causes steric hindrance, while low molecular weight limits inhibition ability. Hence the optimum molecular weight is observed at around 28672 Da with a synthesis pH of IA at 9, and 11 % of initiator. The scale inhibition efficiency reached 81% at a dosage of 10 mg/L. The antiscalants concentration, scale concentration, pH of water, and heating time are the main factors influent scale inhibition performance. Based on the morphology analysis of $CaCO_3$ obtained by scanning electron microscopy (SEM), the mechanism of PIA inhibiting $CaCO_3$ can be explained by two possible mechanisms, i.e., stabilizing particle dispersion and crystal modification. The inhibition performance of PIA is comparable to commercial antiscalants, e.g., polymaleic acid (PMA) and 2-phosphonobutane-1,2,4-tricarboxylic acid (PBTC). However, the developed environmentally friendly bio-based material has a high potential for practical applications.

Keywords: Bio-based polymer, Poly(itaconic acid), Synthesis, Antiscalant, Calcium carbonate scale

ACKNOWLEDGEMENTS

First and foremost, I would like to express my deepest gratitude to my advisor, Assoc. Prof. Pakorn Opaprakasit and my co-advisor Dr. Atitsa Petchsuk, who play an essential role in my research by guiding me until I complete my research during my master's degree. I appreciate their kind encouragement and valuable knowledge. The completion of my thesis would not have been possible without their presence. I would like to express my sincere gratitude to my thesis committee, Asst. Prof. Dr. Chariya Kaewsaneha, for offering wonderful comments and helpful instructions. I would like to thank Prof. Dr. Ikuyoshi Tomita for his valuable advice and comments on this work.

I also thank the TAIST-Tokyo Tech scholarship program and Sirindhorn International Institute of Technology, Thammasat University, for offering scholarships and financial support. Additionally, I would like to thank all my lab mates and seniors at the Functional Advanced Material and Engineering (FAME) for their technical and insightful lab discussions. I thank all members of the school of Integrated Science and Innovation (ISI) for their support in administrative matters.

Finally, I would like to express my gratitude to my family for their support and encouragement, financially and emotionally, during my academic life.

Chakriya Kong

TABLE OF CONTENTS

LIST OF TABLES

LIST OF FIGURES

LIST OF SYMBOLS/ABBREVIATIONS

Symbols/Abbreviations	Terms
APS	Ammonium persulfate
BPO	Benzoyl peroxide
Ca^{2+}	Calcium ion
$CaCO_3$	Calcium carbonate
COOH	Carboxyl group
Da	Daltons
FR	Free radical polymerization
EP	Emulsion polymerization
FTIR	Fourier transform infrared.
GPC	Gel permeation chromatography
^{1}H-NMR	Proton nuclear magnetic resonance
IA	Itaconic acid
ICP- OES	Inductively coupled plasma - optical emission spectroscopy.
KPS	Potassium persulfate
Mw	Molecular weight
NaOH	Sodium hydroxide
O/W	oil in water
PBTC	2-Phosphonobutane-1,2,4-tricarboxylic acid
PIA	Poly(itaconic acid)
PI	Phase Inversion Emulsification
pH	Potential of Hydrogen
PMA	Polymaleic acid homopolymer
PVOH	Polyvinyl alcohol
SEM	Scanning Electron Microscopic
W/O	water in oil

CHAPTER 1
INTRODUCTION

1.1 Background of research

The demand for water treatment facilities has grown significantly in response to the requirement for a higher standard of life toward sustainable development goals. Although many water treatment plants were constructed throughout the area, barriers to treatment performance are often found, resulting in reduced treatment efficiency, high-cost spending, and not being environmentally friendly (H. Y. Li et al., 2006). Scale is one of the significant problems caused by the repeated flow of dissolved salt contained in water. Scales grow in the reservoirs that supply water through the manufacturing process, and they generate material-flow resistance by obstructing reserve osmosis, pipe, and valves, resulting in production loss and some cases, could shut down the operations (Frenkel et al., 2019). Like corrosion issues, scale formation is a complicated issue that needs to be considered in a water treatment plant, cooling system, and desalination system. To address this, antiscalants are compounds designed to prevent the precipitation of crystalline dissolved salts that cause scales. Antiscalants are often utilized in water cooling systems, seawater desalination, and water treatment applications. However, the use of antiscalants derived from fossil-based resources has significant drawbacks since some of them include organophosphates, polyphosphates, and phosphonates, which may promote algae reproduction and induce eutrophication. Even though the other antiscalant generated from polyacrylic and polymaleic acids is less hazardous, it is still non-degradable (Barkade et al., 2020; Chew & Mat, 2015; Suo et al., 2018). Recently, vast interests have been in developing scale deposit inhibitors made from non-phosphorus chemicals that are low toxicity, biodegradable, high efficiency on scale inhibition, and inexpensive.

Itaconic acid (IA), or methylene succinic acid, is an unsaturated dicarboxylic acid derived from biomass fermentation. The substance is non-toxic, renewable, and biodegradable. Because of the advantages of new fermentation technology, the cost of IA production has been reduced, making IA more widely utilized (Cunha da Cruz et al., 2018; Goldberg & Stefan Rokem, 2019; Krull et al., 2017; Wierckx et al., 2020).

Because of its chemical nature, IA is replacing petrochemical-based monomers in various applications. IA is utilized in the production of homopolymers and copolymers. Meanwhile, a few research has shown that poly(itaconic acid) is efficient in inhibiting scale formation, such as calcium carbonate, calcium phosphate, and calcium sulfate scales (Cui & Zhang, 2019; Z. Liu et al., 2019). Hence, the emphasis of this research is on the synthesis and characterization of poly(itaconic acid) as a bio-based antiscalant that is both ecologically benign and very effective in preventing scale depositions. The effect of pH, antiscalant dose, scale dose, and molecular weight on the antiscalant's performance is explored and addressed. Finally, optimal reaction conditions in synthesizing poly(itaconic acid) are revealed.

1.2 Objectives

This research aims to synthesize poly(itaconic acid) as a biobased antiscalant. A primary objective of this work is to investigate a suitable method to synthesis the homopolymer of itaconic acid. Then an appropriate method is selected. The major factors that affect the monomer conversion, molecular weight, and scale inhibition performance are examined. The detailed purpose of this study is summarized below.

(i) To synthesize poly(itaconic acid) by free radical polymerization

(ii) To investigate the effect of neutralization of IA in different pH and the effect of initiator concentration on the chemical structures (FTIR), monomer conversion (^{1}H-NMR), and molecular weight (GPC).

(iii) To determine the antiscalant performance of the synthesized PIA on $CaCO_3$

(iv) To study the impact of antiscalant concentration, scale concentration, pH of water, and heating time on the antiscalant performance.

(v) To study the morphology and mechanisms of PIA on Ca scale inhibition.

1.3 Scopes of study

The research is conducted with commercial itaconic acid. Poly(itaconic acid) is synthesized by three different methods, and a method with a high monomer conversion rate will be studied under different conditions, including neutralization of IA and initiator concentration. Then the synthesized poly(itaconic acid) is applied as antiscalant or scale inhibition. Inhibitor concentration, scale concentration, pH of water,

and heating time are selected to investigate as the main factors that affect the inhibition performance. Only effective material is selected to study the inhibition mechanism and morphology based on SEM observation. Two commercial antiscalants, i.e., 2-phosphonobutane-1,2,4- tricarboxylic acid (PBTC) and polymaleic acid homopolymer (PMA) are selected to investigate the scale inhibition efficiency compared with the synthesized materials.

CHAPTER 2
REVIEW OF LITERATURE

2.1 Overview of Itaconic acid

Itaconic acid (IA) is a kind of unsaturated dicarboxylic acid biologically produced from renewable resources by the fermentation of *Aspergillus terreus.* Itaconic acid, or methylene succinic acid, was first discovered in 1837 as a byproduct of the pyrolytic distillation of citric acid, in which, during the distillation of citric acid, three acid types were produced, i.e., itaconic acid, citraconic, and mesaconic acid. The crystalline powder of IA is white colorless and is often soluble in water, ethanol, and acetone, while other properties of IA are shown in **Table 2.1**. The chemical structure of the IA molecule is conjugated with a double bond and contains two carboxylic groups (Goldberg & Stefan Rokem, 2019). In addition, IA is a non-toxic and quickly degradable material (Shi et al., 2017). IA is a sustainable monomer because it is fermented from biomass products, especially glucose and sucrose provide the maximum yields in producing IA. The pH value is the most important factor in determining IA productive yield. Previously, there was not much IA due to the inconvenient synthesis of IA with the low yield. To date, IA is synthesized and used in various applications, including medicine, lubricants, cosmetics, thickeners, and herbicides. Due to the advantage of innovative fermentation technology, the price of IA production has decreased, making IA more universally used.

Table 2.1 The properties of Itaconic acid.

Description	About Itaconic acid	References
Chemical formula	$C_5H_6O_4$	(Scientific, 2022)
Melting point	165-168 ℃	(Kirimura et al., 2011)
Boiling point	268 ℃	(Sriariyanun et al., 2019)
Molecular weight	130.1 g/mol	(Scientific, 2022)
Solubility	83.1g/L	(Sriariyanun et al., 2019)
Density (20℃)	1.63	(da Cruz et al., 2017)

Itaconic acid is not only used as a monomer of poly(itaconic acid) or its copolymers, but it has a modest market as a monomer of many other materials. For example, IA can be used with diamines to synthesize polyamide (Asif.A & Kaneko, 2017), and combined with diols to be polyesters. (Dai et al., 2015). Based on the information, as detailed in **Figure 2.1**, the utilization of IA is widely used in various applications.

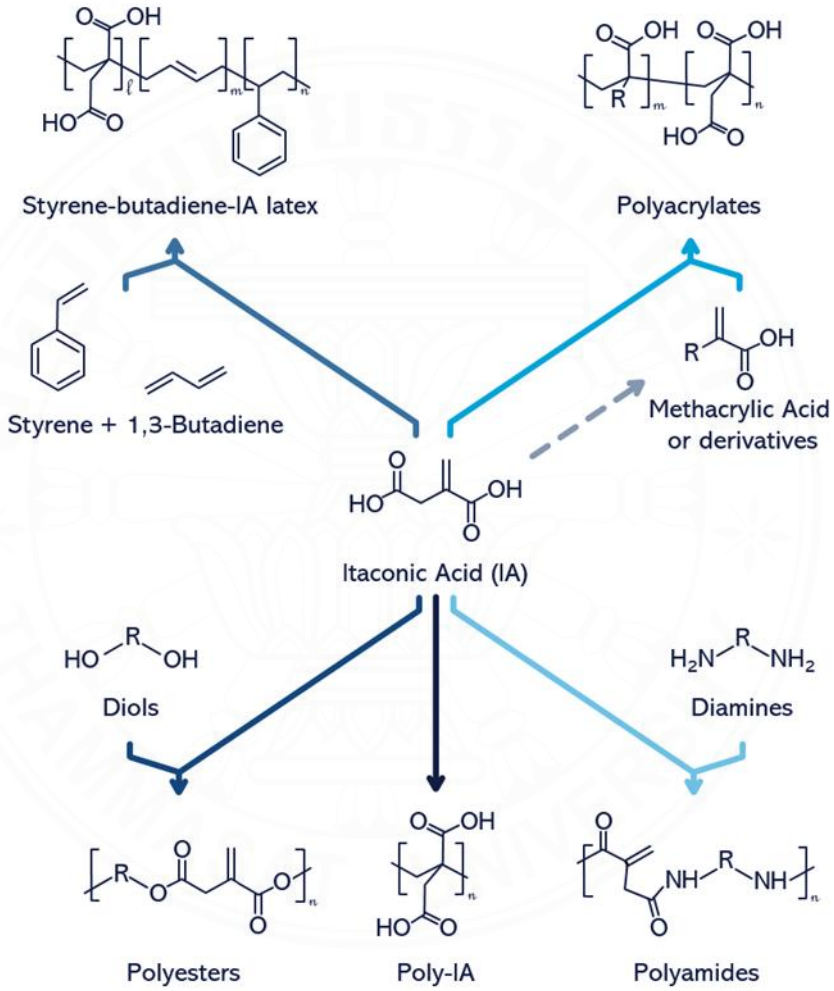

Figure 2.1 The possible conversion of itaconic acid to (co)polymer of new materials.

2.2 Poly(itaconic acid)

Poly(itaconic acid) or PIA is synthesized from the itaconic acid monomer. Previously, the problematic direct polymerization of IA was unsuccessful because of a poor yield. Recently, some PIA has been synthesized and applied in various non-food applications, such as pharmaceuticals, lubricants, cosmetics, thickeners, and herbicides.

Although there are various techniques for synthesizing poly(itaconic acid), including free radical polymerization, condensation polymerization, and solution polymerization, most of them still provide a low conversion (Cao, 2008c). Due to this problem, most of the research has focused on copolymers of itaconic acid with other materials, and itaconic acid homopolymer information is still lacking.

The biodegradability and renewability of poly(itaconic acid) have lately attracted the attention of numerous researchers. Not only the polymerization of IA, but the copolymer of IA is also hugely discussed in current research. As PIA possesses of many excellent properties, many authors discussed the application of PIA to take their benefit into human real life (Abdel-Aziz, 2011; Joy Bell & Subhashini, 2018; Kulal & Badalamoole, 2021; Mohammadinezhad et al., 2018; Sirviö et al., 2021). The polymerization of IA and copolymers of IA play an important role in water treatment applications and are specially described as scale inhibitors (Shi et al., 2017). The molecule of IA contains a carbon double bond as a functional group, which is required for free radical polymerization, and two carboxylic acid groups side by side with the double bond, giving the polymer exceptional negative dispersion and the ability to interact with other ions that cause the scale.

2.2.1 Existing technique for polymerization of poly(itaconic acid)

IA monomer is commonly utilized in the production of polymers by polycondensation or free radical polymerization due to the presence of two carboxylic groups and a vinyl group. Although many studies have been conducted on itaconic polymerization, most have concentrated on itaconic acid copolymers with other materials. However, the homo polymerization of itaconic acid can be done by solution polymerization (Erbil & Uyank, 2001). When persulfate is used as an initiator, the conversion of monomer to polymer is approximately 35% in 68 hours at 50 ℃. However, another study used the same method at 60 ℃ with a polymerization time of 3 days; the conversion was lower than 10% (Cao, 2008c).

A polymerization process has been developed to synthesize homo polymer of poly(itaconic acid) using free radical polymerization. This method is frequently utilized for the polymerization of monomers which consist of carbon double bonds, and the essential chemical in this process is monomer and initiator. A common initiator is

potassium persulfate ($K_2S_2O_8$) or (KPS). Generally, free radical polymerization includes three main steps. Initiation is a stage in which free radical is generated, while propagation is the next stage in which the monomer produces free radical polymerization chains. A termination step is the final stage to end the polymerization. The polymerization of itaconic acid by this method is studied and used as bio-based superabsorbent material (Choi et al., 2022) (Bednarz et al., 2015). The synthesis route of poly(itaconic acid) is shown in **Figure 2.2**

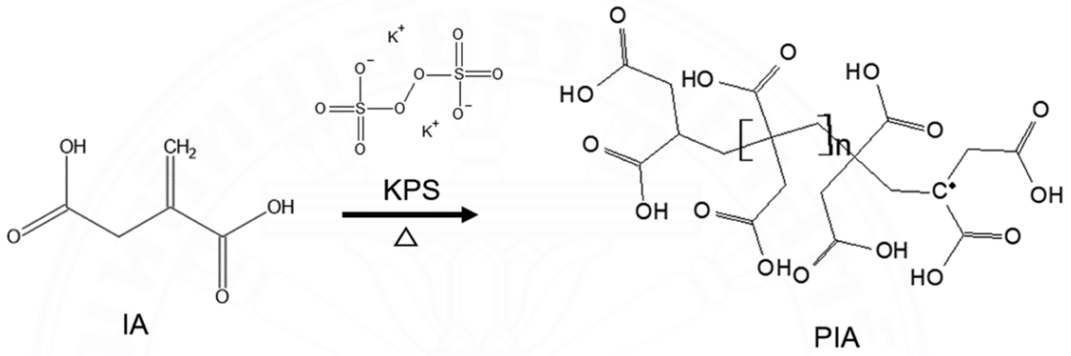

Figure 2.2 The synthesis route of poly(itaconic acid) (Choi et al., 2022)

2.2.2 Structure changes of PIA during polymerization

Poly(itaconic acid) was synthesized as a homopolymer by solution polymerization with high conversion and molecular weight. (Cao, 2008a). This utilized 70 % of tert-Butyl Hydroperoxide (tBHP) as the initiator. The special part of this research study is neutralizing IA by NaOH before polymerization. In addition, the authors pointed out that the neutralizing step is utilized to prevent IA from decarboxylation. However, the heat generated during the addition of NaOH combined with the high temperature in polymerization forced the IA structure, especially the double bond, to form other resonance structures, generating citraconic acid, and (less than 1%) mesaconc acid, which is the trans structure of citraconic acid. This is summarized in **Figure 2.3**.

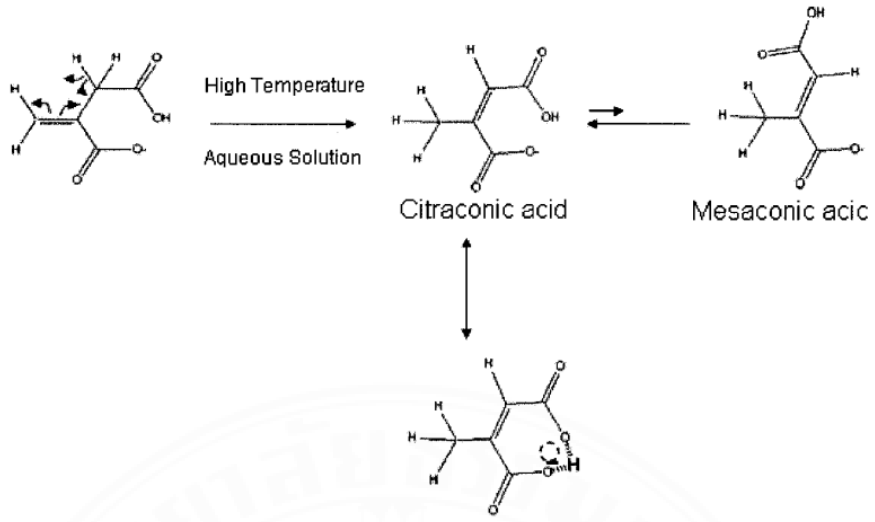

Figure 2.3 The structure change of IA to citraconic acid and mesaconic acid during heating.

Another study investigated the primary structure of the PIA side product and the end group during polymerization. The homo poly(itaconic acid) was synthesized by free radical polymerization in an aqueous solution at 65 °C, and ammonium persulfate as an initiator. The study concentrated on determining the chemical structure of low-molecular-weight side products and terminal groups. They discovered that the principal oxidation generated during free radical polymerization with initiator ammonium persulfate was 2-hydroxyparaconic (HP), itatartaric acid (ITT), acetic acid (AA) and formic acid (FA). While the end group discovered three oligomer distributions consisting of sulfate, hydroxyl, and lactone produced by disproportionation, combination, and transfer, as shown in **Figure 2.4** (Bednarz et al., 2018).

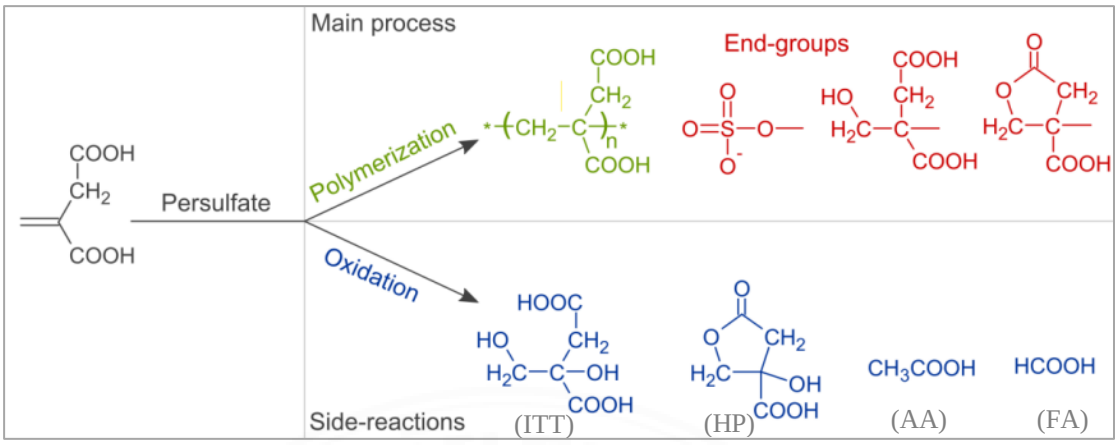

Figure 2.4 The possible oxidation pathway and terminal groups of IA during persulfate-initiated free radical polymerization (Bednarz et al., 2018).

2.2.3 Available methods for synthesizing poly(itaconic acid)

Phase inversion emulsification (PIE) is a process of interconversion between an organic phase, called the oil phase, and another inorganic phase, the aqueous phase. PIE is an emulsion process that uses minimal energy to produce a narrow particle size distribution (A. Kumar et al., 2015). This phenomenon is extensively applied in cosmetic and pharmacological applications, cleaning solvents, etc. This procedure is divided into two basic categories: water in oil (w/o) and oil in water (o/w) (Thananukul et al., 2018). Although this technology is wildly employed in many studies, the mechanism involving it in creating nanoparticles is still uncertain (Preziosi et al., 2013), (M. Kumar et al., 2019). Additionally, The crucial volume ratio that makes phase inversion is known as the emulsion inversion point (EIP), (Bouchama et al., 2003).

PIE has been used to synthesize various materials, for example, poly(lactic acid-co-glycidyl methacrylate) (W. Liu et al., 2006; Thananukul et al., 2018). Various factors impact the material behavior, and one of those parameters is the surfactant concentration. Consequently, the coexistence of surfactant and co-surfactant may control the particle size distribution and prevent particle aggregation. When the surfactant concentration was increased, the particle size distribution became narrow, while the particle size of the material would be broad in the absence of surfactant. Furthermore, the aqueous addition rate impacts the particle of material. Likewise, the rate of stirring during heating might influence particle size distribution.

2.3 Poly(itaconic acid) copolymers

2.3.1 Poly(itaconic acid-co-epoxysuccinic acid)

The copolymer of itaconic acid with other materials is well-known for many applications. The copolymer is possibly produced under the free radical polymerization of IA (Cao, 2008a). This method is widely utilized, and water is preferred as the medium over organic solvents. In addition, this method is often used with the presence of initiator residues and generally uses the aqueous media due to the low-cost spending and non-toxicity. And the use of this initiator is a critical point as well. The synthesis of PIA by this method is convenient and can be used in many applications, including detergent additives, antiscalants, and dispersing agents (Cao, 2008c). For instance, Wenyan et al., synthesized poly(itaconic acid-co-epoxysuccinic acid) (PIA-co-ESA) by free radical polymerization to be a scale inhibitor. And the synthesis equation under this method is demonstrated in **Figure 2.5.** The authors used this copolymer as an antiscalant in water treatment applications. Additionally, they demonstrated various factors that impact antiscalant effectiveness, such as initiator dosage, time, temperature, and monomer ratio. Consequently, the results showed that the best conditions for this material are 11% initiator dosages, 85℃ temperatures, and a monomer ratio of PIA-co-ESA as 4:1 at 4 h. Furthermore, this material is very good at controlling the formation of calcium carbonate scale, with an efficiency rate of 100% within only 18 mg/l (Shi et al., 2017).

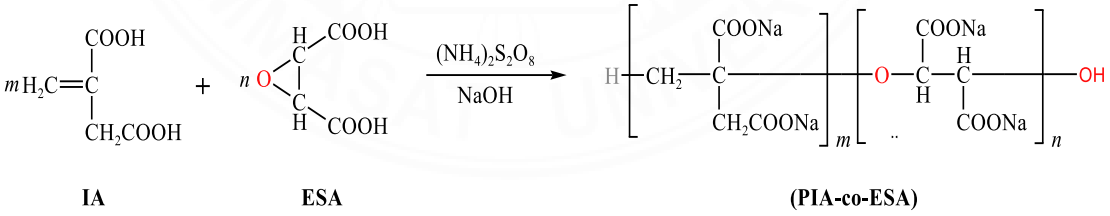

Figure 2.5 Synthesis route of poly (itaconic acid co-expoxysuccinic acid) (Shi et al., 2017)

2.3.2 Suspended Emulsion polymerization Acrylonitrile/Itaconic acid copolymer

The copolymer of IA with other materials is widely developed because IA is a renewable monomer. Hence the copolymer of IA is synthesized to be a useful material for various applications. For example, Mengmeng et al. demonstrated their first study

on the copolymer of IA with acrylonitrile, published in 2008 (Mengmeng et al., 2008). Additionally, the main initiator of this research is potassium peroxydisulfate ($K_2S_2O_8$), while the dispersant agent was poly (vinyl alcohol) (PVA), and the emulsifier was Span80. Otherwise, several factors that influence the average particle size and porosity of synthesis P(AN/IA), including the ratio between monomer and water, the concentration of ($K_2S_2O_8$), (PVA), and span 80 were investigated. Based on the finding indicated that when the mass ratio of water/ monomer was increased, the average particle size was reduced and led to the size distribution being wider. Moreover, increasing the water /monomer ratio could promote porosity more uniform and make the final product more porous with an additional mass water/monomer ratio (Mengmeng et al., 2008). In contrast, the concentration of the initiator had a significant influence on the copolymerization of AN with IA. To ensure that the reaction occurs smoothly, the dosage of KPS must be within a specific range. When the dosage of the initiator increases, the polymerization rate increases and the average particle size decreases, making the target product more uniform.

Nevertheless, the concentration of IA also impacts polymerization as well. The mass of IA needs to be in a range. If the IA concentration exceeds the steric hindrance in the IA structure makes IA more sluggish and decreases the polymerization chain. Whereas increasing PVA and span 80 promote the increase of average particle size. Otherwise, the following conditions were optimized for the AN/IA copolymer preparation: 0.3 :1 for water monomer mass ratio, and the dosage of IA, PVA, KPS, and Span80 were, 12.4, 0.1, 0.5, and 0.5 wt %, depending on the weight of AN individually. The polymerization occurs with an agitation rate of 400 rpm 70 ℃ at 3 hours. The final AN/IA copolymer particle size ranged from 200 to 400μm and the synthesis route is shown in **Figure 2.6** (Devasia et al., 2003).

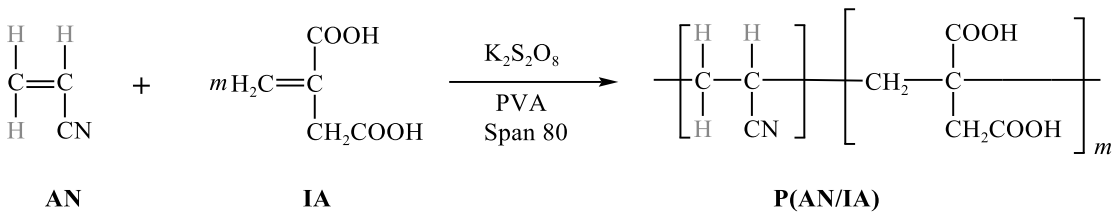

Figure 2.6 Synthesis route of Acrylonitrile/Itaconic Acid Copolymers (Devasia et al., 2003)

2.4 Overview of scale formation

2.4.1 Scale definition

Scale is small precipitations that are frequently found in water. This phenomenon is generated by the presence of dissolved salt, which may react and form white crystals as the scale. Not all the dissolved salt may react and combine to form scale. Generally, scale is formed from salt with less solubility. There are a few common scales that are often discovered, like calcium carbonate, calcium sulfate, calcium phosphate, magnesium silicate, and so on (Shi et al., 2017). Those scales were found and caused economic issues for many industries that use water cooling systems and reverse osmosis treatment. Moreover, the scale can stack on the pipe wall as obtained from **Figure 2.7**, which may damage water treatment equipment, limit its life service, and decrease the efficiency of heat exchange. On the other hand, various factors might impact the growth of scale including alkalinity and acidity or pH, temperature, and the concentration of existing salt in the raw supply. The scale has recently been a prominent issue for many researchers (Barkade et al., 2020; Greenlee et al., 2010; Oshchepkov et al., 2019; Sheng et al., 2020).

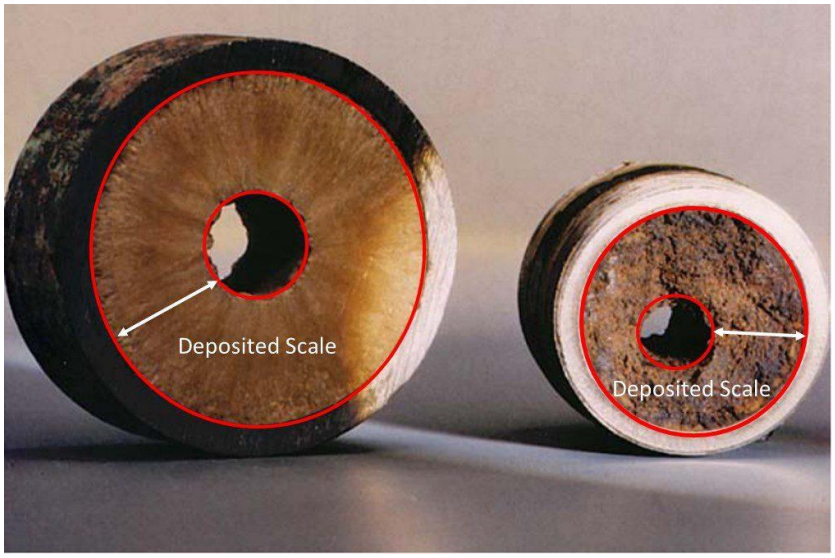

Figure 2.7 The formation of scale deposits in industries' pipe

Although many scale types could be discovered in current industries, the scale's categories are not clearly defined. By the way, the most common scales are sulfide scales, sulfate scales, and carbonate scales (Fink, 2015). The sulfide scale is often found in oil and gas industry pipes, and one scale that is frequently seen is iron sulfide. While

the sulfate scale is often present in seawater, and the most frequent scales observed are barium sulfate (BaSO4) and calcium sulfate (CaSO4) (Jafar Mazumder, 2020). Finally, Carbonate is the most prevalent scale type due to the deposition is occur from CO_2 and free iron in the water. However, ($CaCO_3$) is the most excessive and critical scale, which occurs on all upper layers and inside the apparatus (Jafar Mazumder, 2020).

2.4.2 Characteristics of Calcium carbonate scale

Calcium carbonate is white and odorless with the chemical structure of $CaCO_3$. Calcium carbonate is a natural compound found in every environment, especially in the depth of water in tropical and subtropical environments (Ferreira et al., 2020). Even though calcium carbonate has poor solubility in water and tends to precipitate, adding any ammonium salt or carbon dioxide can increase its solubility in water (Al Omari et al., 2016). Recently, calcium carbonate is a major issue that may impact the efficiency of water treatment and the quality of cooling systems. Since $CaCO_3$ is a common scale that causes on the surface of equipment, it may impact human health if people intake water consisting of calcium carbonate-contaminated water (Bello, 2017).

The reaction equation of forming calcium carbonate (Bello, 2017)

$$CO_{2\,(g)} \leftrightarrows CO_{2\,(aq)}$$

$$CO_{2\,(aq)} + H_2O \leftrightarrows H_2CO_3$$

$$H_2CO_3 \leftrightarrows HCO_3^- + H^+$$

$$HCO_3^- \leftrightarrows CO_3^{2-} + H^+$$

When the calcium ion (Ca^{2+}) is presented in the water. Therefore, $CaCO_3$ is produced as the following equation:

$$Ca^{2+} + CO_3^{2-} \leftrightarrows CaCO_{3\,(s)}$$

Generally, the crystal growth of calcium carbonate is categorized into three basic classes: Vaterite, Aragonite, and Calcite, as shown in **Figure 2.8**. The vaterite is in an unstable state, ready to convert to aragonite and calcite, whereas the calcite is in the most stable state. Based on previous research in $CaCl_2$- Na_2CO_3, the vaterite formation was found at 2-35 ℃, while the aragonite formation is grown at 50 – 70℃.

However, the temperature of 50°C was obtained as an optimum temperature for calcite formation.

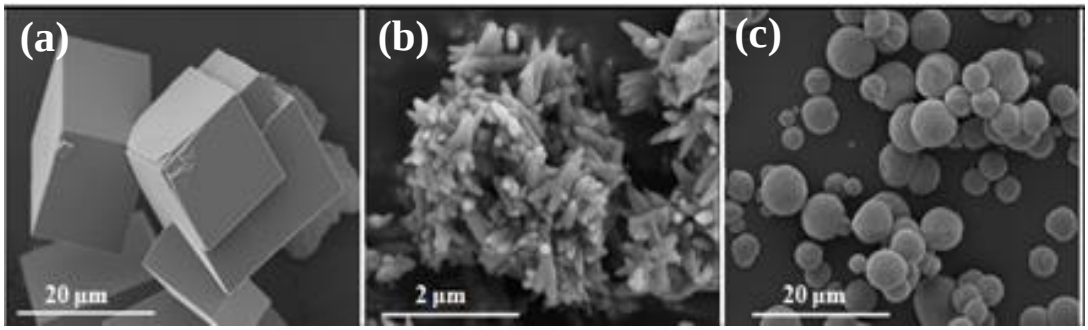

Figure 2.8 The typical shape of calcium carbonate particle. (a) Calcite, (b) Aragonite, (c) Vaterite (Salomão et al., 2017)

2.5 Mechanism of scale formation

Based on the mechanism of scale formation, the growing stage of scale deposit is categorized into three basic stages such as supersaturation, nucleation, and crystal growth as illustrated in **Figure 2.9.**

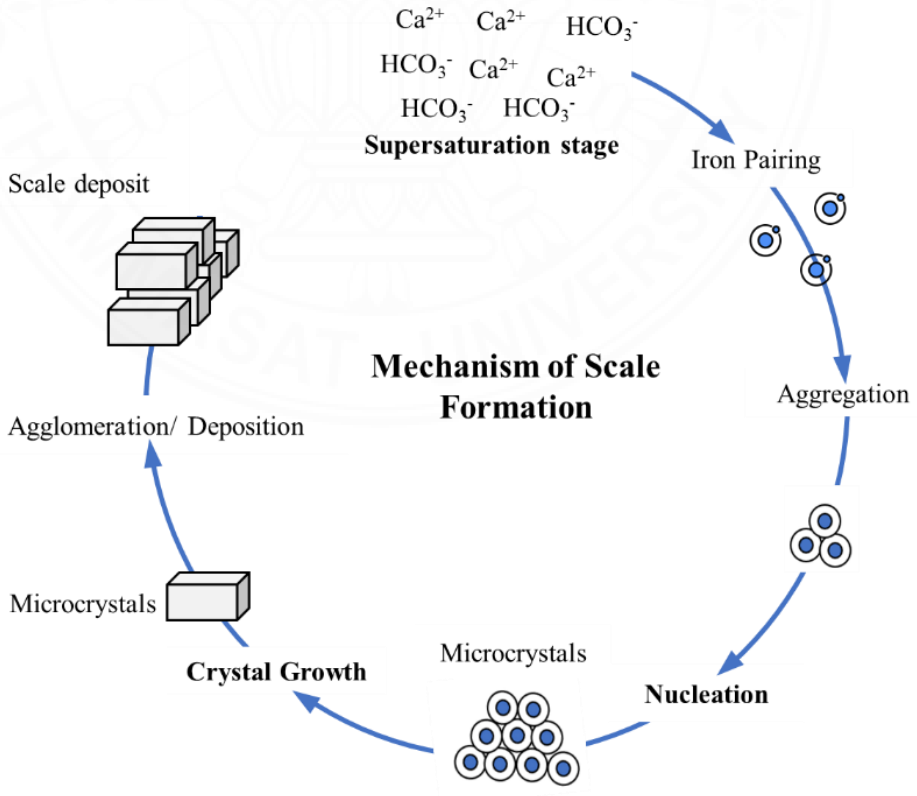

Figure 2.9 The pathway stage of scale formation (Duggirala, 2005)

2.5.1 Supersaturation stage

The first step, known as supersaturation, is the beginning of scale formation, created by the interaction of free soluble cationic and anionic. The opposing ion attempts to form a micro-aggregation via pairing. Many factors may impact this stage, including temperature, scale concentration, surface coating, substance, and roughness. For example, when the concentration of free-scale ions is raised, micro-aggregation is also increased (Al Omari et al., 2016).

2.5.2 Nucleation stage

During the nucleation step, invisible, micro aggregates are formed and grown to a critical size, making the smallest particle insoluble in water. This is an important step in the crystallization of scale deposits, and scale formation preferentially occurs on the surface layer. Moreover, micro aggregation grows continuously in the supersaturation solution while the particle grows. Two different kinds of nucleation processes are often mentioned. When there is no crystallization, primary nucleation occurs, and it usually grows naturally or is induced by another foreign particle. The spontaneous scale formation is known as homogeneous nucleation, which occurs without outside particles and results in a uniform solid. Homogenous nucleation often occurs in a high concentration of supersaturation Whereas, heterogenous nucleation occurs in the presence of foreign particles. In addition, heterogeneous nucleation is more commonly found than homogenous nucleation. At the same time, secondary nucleation happens when there is the existence of a pre-crystal. This stage is automatic to heterogenous nucleation, which is induced by the exited crystal (Bello, 2017; Hoang, 2015).

2.5.3 Crystal growth stage

The crystal growth stage is essential for crystallization growth, which consists of the addition of a new free ion molecule and repeats the formation. However, this stage develops from the critical size of micro aggregation to a large particle that is visible on the surface layer. The mechanism of crystal growth is often studied with a few theories (Bello, 2017; Hoang, 2015). In the theory of surface, energy explained that the scale is growth related to the free surface energy, which may be formed by the

proportion of their surface of energy. While the theory of the adsorption layer explains that crystal growth is dependent on the adsorbed layer of the solute that maybe attaches to the surface of the crystal face, the diffusion theory explains that the growth is based on the diffusion process, and different concentrations of the solution, where solute molecules were transported to the crystal (Bello, 2017).

2.6 Impact of scale on industrial performance

Scale deposition is the precipitation of dissolved salt that grows on the surface layer. The scale has lately been detected in many industries and causes major concern among many manufacturers. Scale is often found in water applications such as reverse osmosis of water treatment facilities and desalination plants and even in cooling systems (Oshchepkov et al., 2019). While excess scale in the water treatment facility affected treatment performance and equipment life, the main problem for manufacturers is high-cost consumption (H. Y. Li et al., 2006). In addition, the rising scale deposit, typically calcium carbonate and calcium sulfate, causes a stick on the filter layer in reverse osmosis and reduces treatment productivity. Moreover, since cooling systems often employ pipelines to manage water flow, an excess of scale deposition may create a crucial barrier by producing crystal growth within the surface layer of the pipeline, resulting in clogging, and lowering heat exchange efficiency. Consequently, it decreases the smooth functioning of equipment and creates an enormous economic loss. Thus, this negative phenomenon is widely interesting for much research to develop the prevention process.

2.7 Overview about antiscalant

Antiscalants, also known as scale inhibitors, are chemical agents designed to prevent the crystallization of dissolved salts or minerals, which might result in scale deposition. Many different antiscalants are frequently employed in water treatment plants, desalination plants, and even cooling systems. Previously, antiscalants were derived from phosphorus compounds. However, that material is still not satisfied due to the bad impact of eutrophication as a part of the environmental impact (Shi et al., 2017). Then the antiscalant is developed with a few criteria such as high efficiency to

inhibit scale, less toxicity, degradable, and especially low cost. However, the antiscalant found in the recent literature review is present ed in **Table 2.2**

Table 2.2 The common compound of existing antiscalant

Compound	Reference
▪ Maleic anhydride /2-acrylanmido-2-methypropanesulfonic acid/ 3-allyloxy-2-hydroxy-1-propanesulfonate (MA/AMPS/AHPSE)	(Yang et al., 2017)
▪ Poly (itaconic acid-co-epoxy succinic acid)	(Shi et al., 2017)
▪ Aminotris (methylenephosphonic acid) (ATMP), 1-hydroxyethane-1,1 diphosphonic acid (HEDP), polyacrylate (PA), copolymer of acrylic and allylsulfonic acids (PAC)	(Kakurkin et al., 2019)
▪ Ter-copolymer of maleic anhydride (MA), 2-acrylamido-2-methylpropanesulfonic acid (AMPS) and hydroxypropyl acrylate (HPA) - P(MA-AMPS-HPA).	(Zhou et al., 2020)

2.7.1 Mechanism of antiscalant

The exact mechanism of antiscalant is not widely determined due to the complication between each mode of antiscalant. But the common mode of antiscalants mechanisms is threshold inhibition, dispersion, and crystal modification. However, an antiscalant could have one mechanism mode or more than that. As shown in **Figure 2.10** in the diagram below, the antiscalant is applied while the scale nucleation is growing microcrystals (Duggirala, 2005).

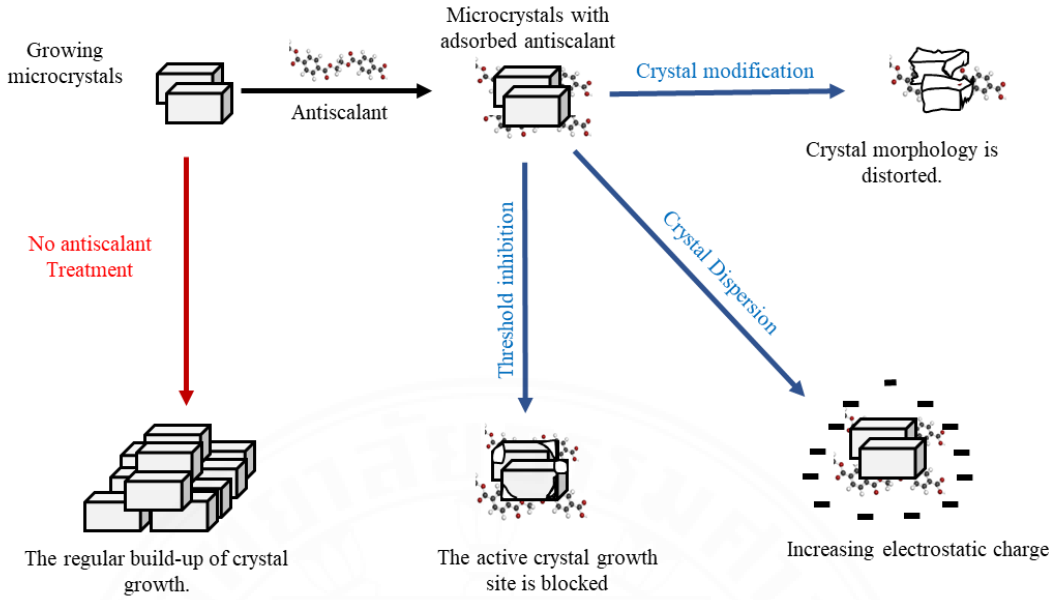

Figure 2.10 The common mechanism pathway of scale inhibition (Duggirala, 2005).

The mechanism of threshold inhibition occurs when the adsorbed antiscalant agent inhibits the formation since the early stage of nucleation, suppresses ion aggregation, and blocks the active crystal growth site of scale. As a result, it inhibited the further formation of the regular crystalline, and the scale formation was minimized. In contrast, the dispersion mechanism is achieved when the antiscalant is adapted to the growing microcrystal and prevents aggregation by increasing the anionic charge on the scale surface (Duggirala, 2005). The exceeded electrostatic repulsive force between microcrystals could prevent further growth of scale by the negative charge adhering scale layer from the formation. The crystal modification mechanism occurs when adsorbed antiscalant changes the morphology of the formation microcrystal to be unusual form. In contrast, the destroyed formation leads to minimizing the scale of crystalline (Singh & Ng, 2019).

Although the mechanism of poly(itaconic acid) is not clearly identified, a study demonstrated that PIA is threshold scale inhibition (Stanley Walter & James William, 1983). PIA is not different from other antiscalants with the numerous presences of the carboxylic acid group (COOH), which is the essential part that could inhibit scale formation (J. Li et al., 2016; Zhao et al., 2021). The deprotonate of COO^- captures free

Ca^{2+} ions, which are the origin of scale formation. The general mechanism of PIA is detailed in **Figure 2.11**.

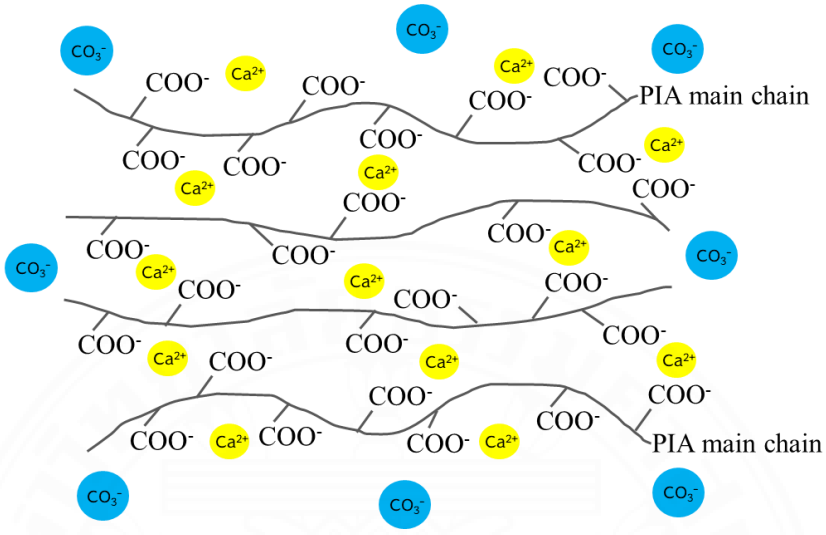

Figure 2.11 Mechanism of poly (itaconic acid) on calcium carbonate

2.8 Factors influent on antiscalant performance

The efficiency performance of an antiscalant is dependent on several factors, such as the pH of water, the compound of the antiscalant, the molecular weight of antiscalants, the concentration of the antiscalants, etc.

2.8.1 pH of water

The various sources of water might produce a different range of pH. In surface water, the pH ranges from 6.5 to 8.5, whereas in groundwater, the pH is 6 to 8.5. Furthermore, the average pH of the water-cooling system is 8 to 10 (Filtration, 2022). According to WHO guidelines, the average pH of drinking water should be 6.5 to 8.5 (World Health Organisation, 2007). However, the difference in water pH could affect antiscalant performance (X. Li et al., 2015). For example, the antiscalant produced from a group of maleic anhydrides (MA), 2-acrylamido-2-methylpropanesulphonic acid (AMPS), and 3-allyloxy-2- hydroxy-1-propanesulfonate (AHPSE) or MA/AMPS/ AHPSE is conducted with the various pH range from 7 to 10. The consequence illustrated that in lower pH, the efficiency of antiscalant performance is better in a lower pH, as presented in **Figure 2.12** (Yang et al., 2017). This phenomenon might be caused

by the fact that the higher pH is the preference for flocculation and scale formation (Huang et al., 2019; Luo et al., 2015).

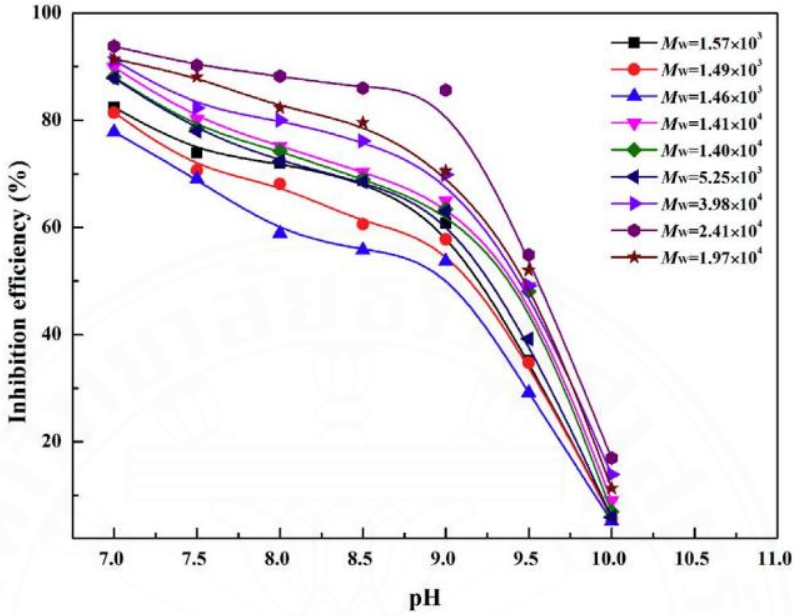

Figure 2.12 The influence of pH on scale inhibition efficiency (Yang et al., 2017)

2.8.2 Compound of antiscalant

Antiscalant is developed from several types of material, but most of them are polymers. And the chemical composition of antiscalant polymer impacts their ability to prevent scale deposits. For example, the copolymer of maleic and acrylic acid (MA-AA) has a better scale inhibition efficiency than polyacrylic acid sodium salt (PAAS). Since the duplicate carboxylate group in MA-AA copolymer structure promotes the inhibition of scale formation more than the single carboxylate group in the structure of PAAS (Popov et al., 2016). However, the end group of antiscalant composition has a considerable influence on crystallization. The end group of polymers could influence the absorption of scale formation. Polymers with hydrophilic end groups are the most efficient in inhibiting scale development, whereas polymers with hydrophobic end groups are the least effective (Kiran D. Dhawale, Nitin M. Thorat, 2018). **Table 2.3** summarizes the information on antiscalants that exist in current research:

Table 2.3 The chemical structure of existing antiscalants.

Antiscalants	Chemical structure	References
Poly(maleic acid)	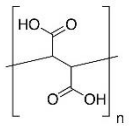	(Chew & Mat, 2015)
Poly(acrylamide)	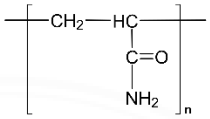	(Zhang et al., 2017)
Poly(acrylate) (PA)	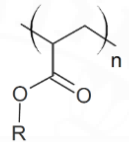	(Kakurkin et al., 2019)
Polyacrylic acid (PAA)	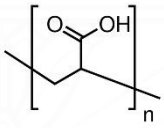	(Kakurkin et al., 2019)
Polyaspartic acid (PASP)	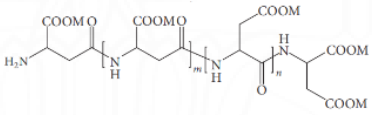	(Amjad & Koutsoukos, 2014)
Maleic and acrylic acid copolymer (MA-AA)	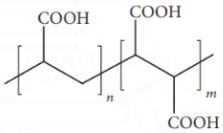	(Popov et al., 2016)
Aminotris (methylene-phosphonic acid) (ATMP)	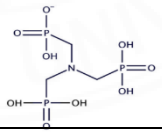	(Kakurkin et al., 2019)

2.8.3 The molecular weight of antiscalant

Besides the antiscalant composition, another essential factor that influences antiscalant performance is the molecular weight (Mw) of the antiscalant. A few research have been studied to determine the impact of Mw of material on antiscalant performance. For instance, in the constant concentration chemical structure and pH, the inhibition percentage of MA/AMPS/AHPSE combat with calcium carbonate provides the greatest performance when the molecular weight reaches 24100 Da. In contrast, the

lower molecular weight (Mw is 1490) and higher molecular weight (Mw is 39800) might decrease the inhibition percentage, as mentioned in **Figure 2.13** (Yang et al., 2017). In addition, another author also demonstrates the performance of molecular weight of several materials, including poly (maleic acid), poly(acrylamide), poly (acrylic acid), poly(methacrylic acid), poly (vinyl pyrrolidone), poly(2-acrylamido 2-methylpropane sulfonic acid), etc. And the best performance is provided by the poly (maleic acid) with a lower molecular weight (Amjad & Koutsoukos, 2014).

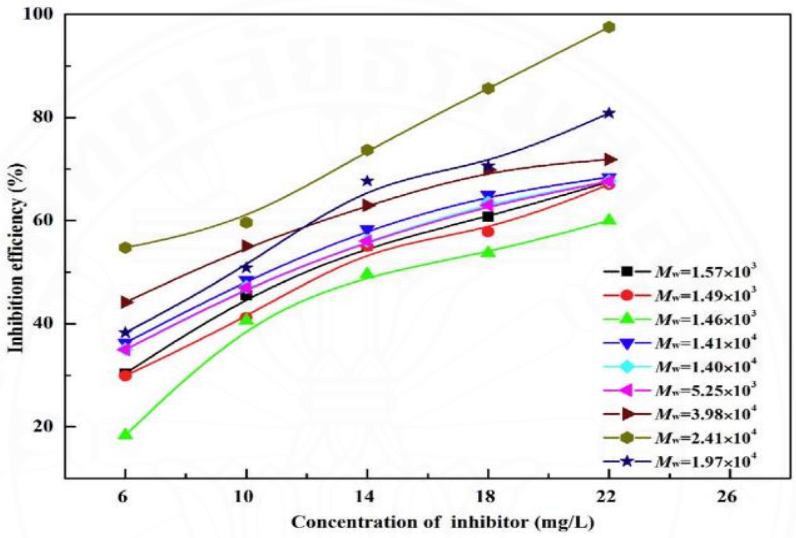

Figure 2.13 The chemical structure of existing antiscalants

2.8.4 Concentration of antiscalant

The concentration or dosage of antiscalant could promote the effectiveness of scale inhibition. For example, a researcher investigated the influence of antiscalant concentration ranging from 2-16 mg/L by many repetitions. Consequently, when the antiscalant dosage is minimal, the percentage inhibition improves with increasing antiscalant concentration (H. Li et al., 2007). Once scale inhibitor dosage reaches a threshold, the effectiveness of the antiscalant grows very little or keeps steady with increasing antiscalant concentration (Zhang et al., 2017). Another explanation might be that after the antiscalant has been attached to all active sites on nucleus surfaces, increasing scale inhibitor concentration seems to have an insignificant effect on the scale formation (Tang et al., 2017; Zhao et al., 2021). Furthermore, the utilization of lower-scale inhibition concentration with high-scale performance promotes the economy.

CHAPTER 3
METHODOLOGY

3.1 Materials

The main chemical used for the synthesis of poly(itaconic acid) is itaconic acid (IA) (>99 %) was purchased from Sigma Aldrich. Ammonium persulfate or $(NH4)_2S_2O_8$ (>98%) was supplied by Elago Enterprises. Sodium hydroxide anhydrous (NaOH) (>98%) and potassium sulfate (K_2SO_4) were supplied by Carlo Erba. Polyvinyl alcohol or PVOH $(C_2H_4O)_n$ supplied by Sigma Aldrich, and Sodium dodecyl sulfate or sodium lauryl sulfate or SDS ($NaC_{12}H_{25}SO_4$), benzoyl peroxide or BPO ($C_{14}H_{10}O_4$) chloroform solvent ($CHCl_3$). Additionally, the material used in antiscalant performance are calcium chloride anhydrous ($CaCl_2$) (>90%) and sodium bicarbonate ($NaHCO_3$) (>99.8%) supplied by Carlo Erba. However, commercial antiscalants like polymaleic acid (PMA) and 2- Phosphonobutane-1,2,4-tricarboxylic acid (PBTC) were provided by Water Doctor Co., Ltd. All chemicals were used without further purification.

3.2 Synthesis of poly (itaconic acid)

3.2.1 Synthesis of PIA by Emulsion polymerization

The homopolymer of itaconic acid can be synthesized in various polymerization techniques. PIA is synthesized using the conventional method, which is emulsion polymerization. To get the target material, the mixture of 5 g of IA, 2% w/v of potassium sulfate (K_2SO_4), 2 % w/v of PVOH $(C_2H_4O)_n$, 2% w/v of SDS ($NaC_{12}H_{25}SO_4$), and 30 mol % w/v sodium hydroxide (NaOH) with a certain amount of distilled water was added in the 250 ml round flask. Under the nitrogen atmosphere, the mixture was stirred at 500 rpm and heated up to 80 ℃ with a polymerization time of 4 hours. Then PIA is synthesized and formed as a slightly yellow solution and labeled as EP-N30. The synthesis pathway is detailed in **Figure 3.1**.

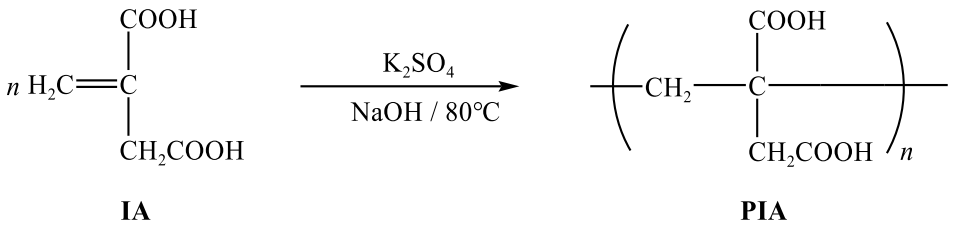

Figure 3.1 The synthesis route of EP-N30

3.2.2 Synthesis of PIA by Phase Inversion polymerization

PIA is prepared by phase inversion emulsification, which prepares by the oil phase and aqueous phase. In the oil phase, a certain amount of itaconic acid and 4% of BPO ($C_{14}H_{10}O_4$) as initiator, 2% of PVOH $(C_2H_4O)_n$ as a surfactant, and 30 mol % of NaOH as neutralizer were dissolved in chloroform solvent ($CHCl_3$). In contrast, the aqueous phase is prepared by dissolving the 2% w/v of SDS ($NaC_{12}H_{25}SO_4$) as a co-surfactant into 50 ml of distilling water. After the mixture of the aqueous phase was completely dissolved, it was dropped slowly into the oil phase substance. During that time, the polymerization solution was stirred under a magnetic stirrer at 500 rpm under a nitrogen atmosphere. In addition, the reaction was heated to 80 ℃ and maintained for 4 hours as a polymerization time. This PIA was labeled as PI-N30. Nevertheless, the route of a homopolymer of itaconic acid is shown in **Figure 3.2**.

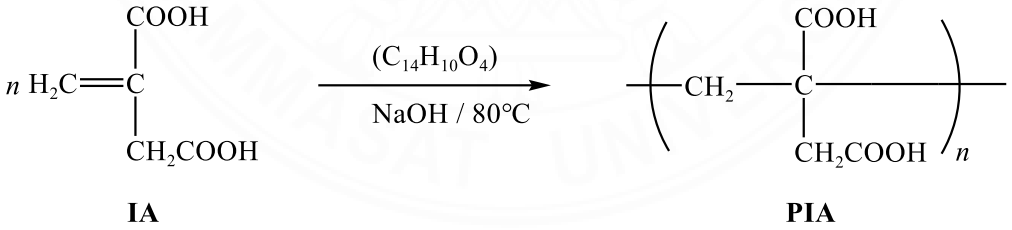

Figure 3.2 The synthesis route of PI-N30

3.2.3 Synthesis of PIA by Free radical polymerization

3.2.3.1 Synthesis of PIA by neutralizing IA in different pH

Poly (itaconic acid) is synthesized by free radical polymerization by preparation of 5 g of itaconic acid with a certain amount of deionized water mixed in a 250-ml round-bottom flask with the constant speed of a mechanical stirrer. This condition focused on the neutralizing of IA before the polymerization. Hence, 50 % of sodium

hydroxide (NaOH) is added to IA to get the exact pH like pH4, pH5, pH7, and pH9. Then they were labeled as FR-PH4, FR-PH5, FR-PH7, and FR-PH9, respectively. After that, the 11% of initiator ammonium persulfate $(NH_4)_2S_2O_8$ is dissolved in 10 ml of deionized water and dropped slowly into the round flask consisting of the aqueous phase of the monomer. The reaction mixture is heated to 85 ℃ using a heating mantle under a nitrogen atmosphere and maintains the reaction temperature for 4 hours. In the end, the homopolymer of PIA is demonstrated as a slightly yellow solution. Additionally, the pathway of PIA synthesis is shown in **Figure 3.3.**

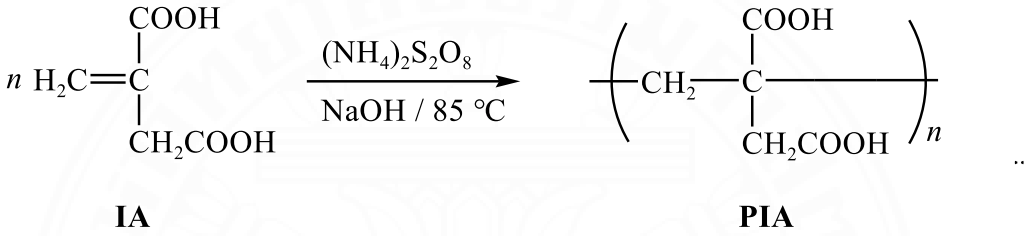

Figure 3.3 The synthesis route of PIA by free radical polymerization

Table 3.1 The summary of PIA samples by variation of pH of IA

Sample code	IA (g)	PH	Initiator (%)	Polymerization condition
FR-PH4	5	4	11	4 h, 85℃
FR-PH5	5	5	11	4 h, 85℃
FR-PH7	5	7	11	4 h, 85℃
FR-PH9	5	9	11	4 h, 85℃

3.2.3.2 Synthesis of PIA by variation of the initiator concentration.

PIA is synthesized by free radical polymerization by preparation of 5 g of itaconic acid with a certain amount of deionized water mixed in a 250-ml round-bottom flask with the constant speed of a mechanical stirrer. Then 50 % of sodium hydroxide (NaOH) is added to neutralize IA until the pH of the solution turns to pH 9. Because this condition concerns the variation of initiator concentration, 5%, 8%, 11%, and 14% of initiator ammonium persulfate $(NH_4)_2S_2O_8$ is dissolved individually in 10 ml of deionized water. Then the initiator solution was dropped slowly into the round flask

containing the monomer's aqueous phase. Then those solution samples were labeled as FR-A5, FR-A8, FR-A11, and FR-A14, respectively, as summarized in **Table 3.2**. The reaction mixture is heated to 85 ℃ using a heating mantle under a nitrogen atmosphere and maintains the reaction temperature for 4 hours. In the end, the homopolymer of PIA is demonstrated as a slightly yellow solution. However, the FR-PH9 is the same as FR-A11 in this variation.

Table 3.2 The summary sample of PIA by variation of initiator concentration

Sample code	IA (g)	PH	Initiator (%)	Polymerization condition
FR-A5	5	9	5	4 h, 85℃
FR-A8	5	9	8	4 h, 85℃
FR-A11	5	9	11	4 h, 85℃
FR-A14	5	9	14	4 h, 85℃

3.3 Characterization of poly (itaconic acid)

3.3.1 Fourier transform infrared spectroscopy analysis.

The chemical structure of PIA is analyzed using Fourier transform infrared (FTIR) spectroscopy. Since the PIA is demonstrated as a slightly yellow transparent solution, the PIA is first dried in the hot air oven at 60 ℃ for 24 h. Then the brittle PIA was ground to be a powder. The measurement of PIA is investigated on wavelength 525 to 4000 cm^{-1} with 32 scans and a resolution of 2 cm^{-1}.

3.3.2 Nuclear magnetic resonance analysis

To determine the PIA structures and the monomer conversion, the proton nuclear magnetic resonance (^{1}H-NMR) spectra were recorded on a Bruker Avance III^{TM} HD 600 MHz. Before measurement, the samples were dried in a vacuum oven at 60 ℃ for 24 h. Then 20 mg of dry samples were completely dissolved in deuterium oxide (D_2O).

The conversion of IA to PIA was calculated based on the following equation:

$$C\% = 1 - \frac{1H_m}{1H_m + H_p}$$

Where H_p is the integral polymer peak at 2.2 to 2.7 ppm.
H_m is the integral monomer peak at 5.3 or 5.7 ppm.

3.3.3 Gel permeation chromatography analysis

The molecular weight of the material was measured using gel permeation chromatography (GPC) with a Water 2414 refractive index detector on Mw resolving range 10^3 to 7×10^6. Similar to the previous measurement, PIA was first dried at 60 °C for 24 h. The samples were stirred overnight for complete dissolution, then filtered using nylon 66 membrane with pore sized 0.45 μm before injection. The eluent was 0.05M of sodium bicarbonate buffer (pH 11) at 30°C, with a flow rate of 0.6ml/min. And the injection volume is 20 μl. In addition, the average molecular weight of the sample was calculated based on the following equation:

$$\bar{M}_w = \sum_{i=1}^{n} A_i \,.\, M_{wi}$$

Where A_i: mole fraction of i.
M_{wi}: the molecular weight of i.

3.4 Evaluation of antiscalant performance on $CaCO_3$ inhibition

3.4.1 Synthesis brine solution

The formation of scale calcium carbonate is achieved by mixing the two-synthesis brine solution, which is the source of calcium (Ca^{2+}) and bicarbonate (HCO_3^-). To get the free calcium ion, 2.775 g of calcium chloride ($CaCl_2$), and 1.3776 g of sodium bicarbonate ($NaHCO_3$) are separately dissolved in 1 L of distilled water type I to reach the concentration of Ca^{2+} and HCO_3^- to 1000 mg/L. The dissolution is prepared in the Duran laboratory glass bottle under the magnetic stirrer until the brine is

completely dissolved. The solution is left at ambient temperature for a few hours to stabilize the synthesis brine solution.

3.4.2 Antiscalant performance measurement

Calcium carbonate ($CaCO_3$) is the most prevalent scale formation, which causes a huge amount of scale formation in water treatment and cooling systems. To overcome this concern, the performance of PIA is evaluated based on the China National Standard method (GB/T 16632-2008). The ratio volume 1:1 of [Ca^{2+}] and [HCO_3^-] in a concentration of 250 mg/L was combined in the glass test tube. The scale treatment was tested in initial water pH, which was around 7.5-8.0. The pH of treatment following industrial treatment pH in the approximate range 7-10. The scale testing was treated at 80 ℃ in a bio shaker water bath and left this constant temperature for 10 hours. A small-scale formation of calcium carbonate appeared on the surface of the glass test tube. After the treatment tubes were cooled down for two hours, the precipitation was filtered by using Whatman filter paper. Finally, the supernatant, which consists of Ca^{2+} ions, was analyzed using Inductively coupled plasma-optical emission spectrometry (ICP-OES) techniques. The antiscalant efficiency performance of poly (itaconic acid) to suppress with calcium carbonate is determined based on the following equation below:

$$\text{Scale inhibition efficiency } (\%) = \frac{[Ca^{2+}]_{\text{final}} - [Ca^{2+}]_{\text{blank}}}{[Ca^{2+}]_{\text{initial}} - [Ca^{2+}]_{\text{blank}}} \times 100$$

$[Ca^{2+}]_{final}$: is the *final* concentration of Ca^{2+} in the filtrate in the presence of *antiscalant* after 10 hours.

$[Ca^{2+}]_{blank}$: is the *final concentration* of Ca^{2+} in the filtrate without antiscalant after 10 hours.

$[Ca^{2+}]_{initial}$: is the *initial concentration* of Ca^{2+} at the beginning of the experiment without antiscalant.

CHAPTER 4
RESULTS AND DISCUSSION

4.1 Synthesis and Characterize of PIA

4.1.1 The appearance of PIA

The PIA was synthesized by three different methods, including emulsion polymerization (EP), Phase inversion emulsification (PI), and Free radical polymerization (FR). **Figure 4.1** illustrates the appearance of the PIA products synthesized from the three methods. The appearance of PIA is a yellow transparent liquid. EP-N30 refers to PIA synthesized by Emulsion polymerization, PI-N30 refers to PIA synthesized by Phase inversion Emulsification, and FR-PH7 refers to PIA synthesized by Free radical polymerization.

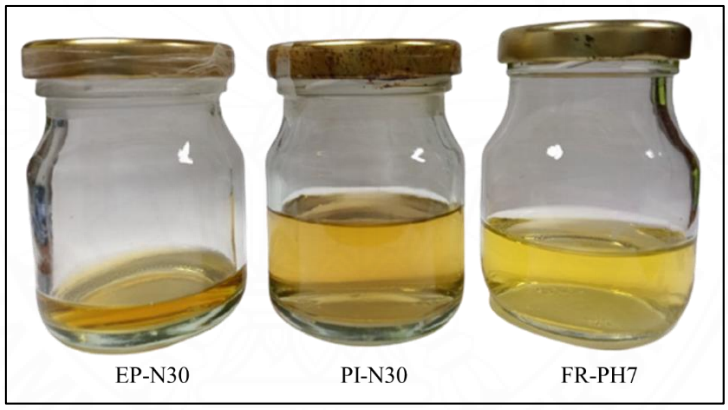

Figure 4.1 The appearance of EP-N30, PI-N30, and FR-PH7

4.1.2 FTIR analysis of PIA

The chemical structures of PIA samples were characterized by using FTIR, as shown in **Figure 4.2**. The purple spectra indicated itaconic acid, while the dark red, light blue, and dark yellow spectra indicated PI-30, EP-N30, and FR-PH7, respectively. IA showed strong peaks at 1683 and 1622 $cm^{-1,}$ corresponding to the C=O stretching vibration of the carboxyl group and the C=C stretching vibration of IA, as described in previous research (Kiran D. Dhawale, Nitin M. Thorat, 2018).

The synthesized PIA from both emulsion polymerization (EP-N30) and phase inversion emulsification (PI-N30) illustrated a strong peak at 1701 $cm^{-1}$and 1687 cm^{-1}

corresponds to the C=O group (Choi et al., 2022). Nevertheless, the lower peak at 1629 cm^{-1} and 1631 cm^{-1} of EP-N30 and PI-N30 correspond to the C=C bond in both spectra, reflecting that the double bond conversion was not completed, and some monomers remained (Cui & Zhang, 2019). The peak~ 1360-1590 cm^{-1} corresponds to the symmetric and asymmetric stretching of carboxylate ion, which gets from the presence of NaOH in both methods. The other remaining peaks indicated the general chemical structure of itaconic acid.

However, the spectrum of FR-PH7 synthesized by free radical polymerization showed a strong peak at 1548 cm^{-1} and 1386 cm^{-1} corresponding to the asymmetric and symmetric carboxylate ion generated from the neutralization step at the beginning of the polymerization (Shi et al., 2017). The disappearance of the C=C band confirmed the complete polymerization.

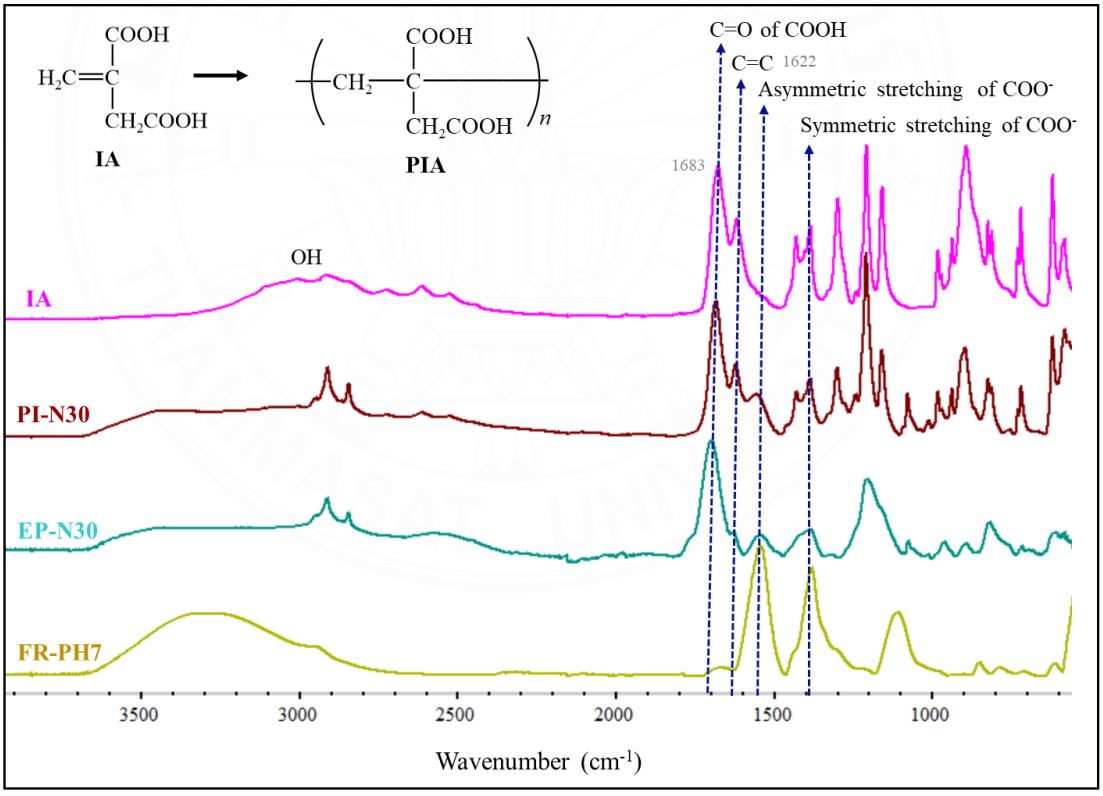

Figure 4.2 FTIR spectra of IA, PI-N30, EP-N30, and FR-PH7

Based on the FTIR analysis of the products from the three methods, FR-PH7, which was synthesized by free radical polymerization, showed an interesting part since its structure consists of a strong COO^-, which can play a major role in scale inhibition.

Additional analyses were continually conducted based on ^{1}H-NMR to determine the monomer conversion.

4.1.3 ^{1}H-NMR and GPC analyses of PIA

The PIA products synthesized by different methods were characterized by ^{1}H-NMR to study their structure. The analysis of PIA by ^{1}H-NMR was obtained at 600 MHz at 25 ℃ in D_2O. **Figure 4.3** shows the spectra of EP-N30, PI-N30, and FR-PH7. The two peaks at 5.3 and 5.7 ppm represented the proton in group CH_2= or (a), and the peak around 3.1 ppm represented CH_2- or (b) inside a group of unreacted itaconic acid (Cummings et al., 2016). In addition, the strong peak at around 4.7 ppm is represented by the solvent D_2O. However, the similar integrals at 2.2 and 2.7 ppm of EP-N30 and PI-N30, and the broad peak at 2.2 ppm and 2.7 ppm of EP-PH7 illustrated the CH_2- in the backbone (c) and side chain (d) of PIA structure (Cao, 2008a). Nevertheless, based on previous research, the beginning triplet peak at 0.9, 1.2, and 1.9 ppm of EP-N30 and PI-N30 showed the CH_3- and CH_2-, which might be caused by the presence of SDS (Malik et al., 2016). And the singlet peak at 3.7 ppm of both spectra indicates the CH- of the PVOH structure (Korbag & Mohamed Saleh, 2016). The presence of SDS and PVOH due to the material is analyzed without purification (Korbag & Mohamed Saleh, 2016). However, the monomer conversion rate of IA to PIA could determine by ^{1}H-NMR and calculated based on the following equation:

$$C\% = 1 - \frac{1H_m}{1H_m + H_p}$$

where H_p is the integral polymer at peak 2.2 to 2.7 ppm

H_m is the integral monomer at peak 5.3 ppm or 5.7 ppm.

Table 4.1 shows the molecular weight, monomer conversion, and pH of the synthesized PIA. The results indicate that the monomer conversion of FR-PH7 has a higher monomer conversion than the other two methods.

Table 4.1 The Mw, monomer conversion, pH of EP-N30, PI-N30, and FR-PH7

Sample	Average Mw (Daltons)	Monomer Conversion (%)	pH of sample
EP-N30	37049	67	3.51
PI-N30	6609	31	3.70
FR-PH7	21380	96	7.53

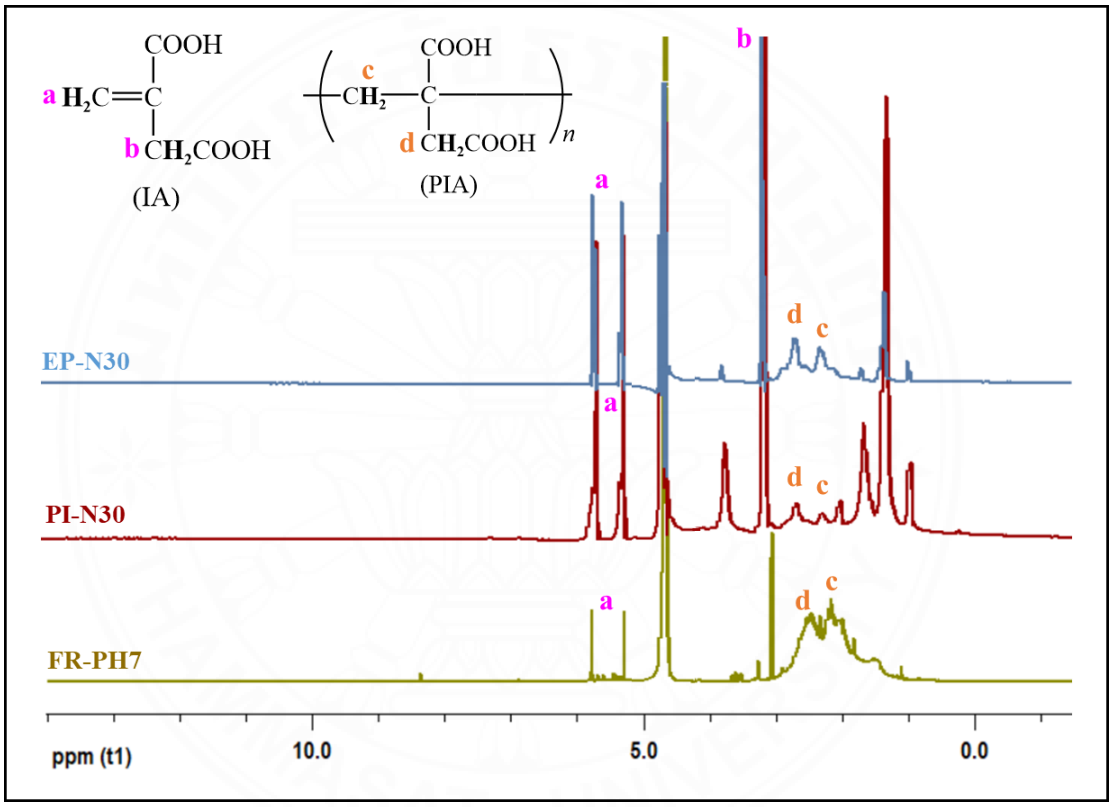

Figure 4.3 ^{1}H-NMR spectra of EP-N30, PI-N30 and FR-PH7

4.1.4 Antiscalant Performance of PIA on $CaCO_3$ scale

The impact of concentrations ranging from 20 to 100 mg/L on antiscalant efficiency of the synthesized PIA was evaluated against calcium carbonate. The scale inhibition efficiency of EP-N30, PI-N30, and FR-PH7 at various concentrations, at the initial pH (pH 7.5-8.0), is shown in **Figure 4.4**. The results indicate that the performance efficiency improved with increasing antiscalant concentration. However, once the antiscalant dose reaches a certain level, the efficiency of the antiscalant keeps steady (Yang et al., 2017).

Based on the finding, the performance of EP-N30 illustrated a poor scale inhibition performance with only 42% at a dosage of 100 mg/L. Whereas PI-N30 demonstrated a considerable increase based on dosage. At a dosage of 20 mg/L, PI-N30 could control the growth of scale deposits by 16 %, while at 100 mg/L, the antiscalant performance improved to 75%. Although the controlling of $CaCO_3$ by using PI-N30 is effective, the PI-N30 consumption is still high. Nevertheless, the FR-PH7 shows an effective scale inhibition. At a dosage of 20 mg/L, the antiscalant performance of FR-PH7 was 70 %. While the optimum efficiency of FR-PH7 reached 82% at a dosage of 60 mg/L. When the efficiency reached the optimum, the inhibition percentage did not increase. In sum, the scale inhibitor performance is decreased following this order: FR-PH7 > PI-N30 > EP-N30.

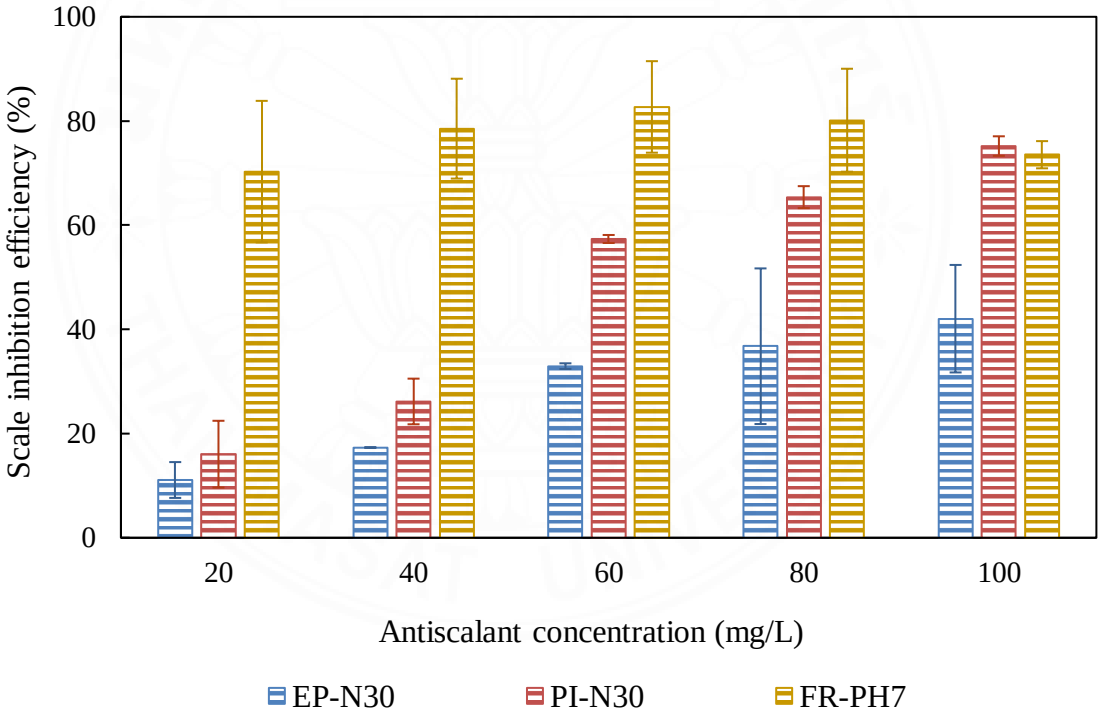

Figure 4.4 The antiscalant performance of EP-N30, PI-N30, and FR-PH7

FR-PH7, synthesized by free radical polymerization, provides the optimum molecular weight and high monomer conversion. The scale inhibition of FR-PH7 illustrated a high inhibition percentage with low concentration consumption. Furthermore, the free radical polymerization method is more convenient and beneficial than emulsion polymerization and phase inversion emulsification. Therefore, the free

radical polymerization method has been chosen for further study under various conditions to improve monomer conversion and antiscalant performance.

4.2 FTIR analysis of PIA by free radical polymerization

4.2.1 Effect of neutralization of IA

In free radical polymerization, the IA solution was neutralized at different pH levels (pH 4,5,7, and 9). IA was analyzed using FTIR to examine the influence of neutralization pH on IA structure. From **Figure 4.5**, IA consists of a carboxylic group, reflected by the bands at 1683 cm^{-1} and double bound at peak 1622 cm^{-1}. At pH 4, IA might neutralize only half of the total (COOH) in its structure, meaning that half of COOH is converted to COONa. This is reflected by the peak at 1557 cm^{-1} corresponding to the carboxylate group (COO^-), while the remaining COOH is represented by the peak at 1683 cm^{-1}. At pH 5, as the pH increases, more IA is neutralized. The FTIR spectrum showed a decrease in the intensity of the peak at 1692 $cm^{-1,}$ corresponding to a decrease in the concentration of COOH and an increase in the concentration of carboxylate at 1560 cm^{-1}. At pH 7 and 9, the IA structure is completely neutralized. The FTIR spectrum shows the absence of a peak corresponding to COOH since all COOH is converted to carboxylate (COO^-) and showed a strong peak at 1560-1568 cm^{-1}. In contrast, the C=C has remained in the IA structure.

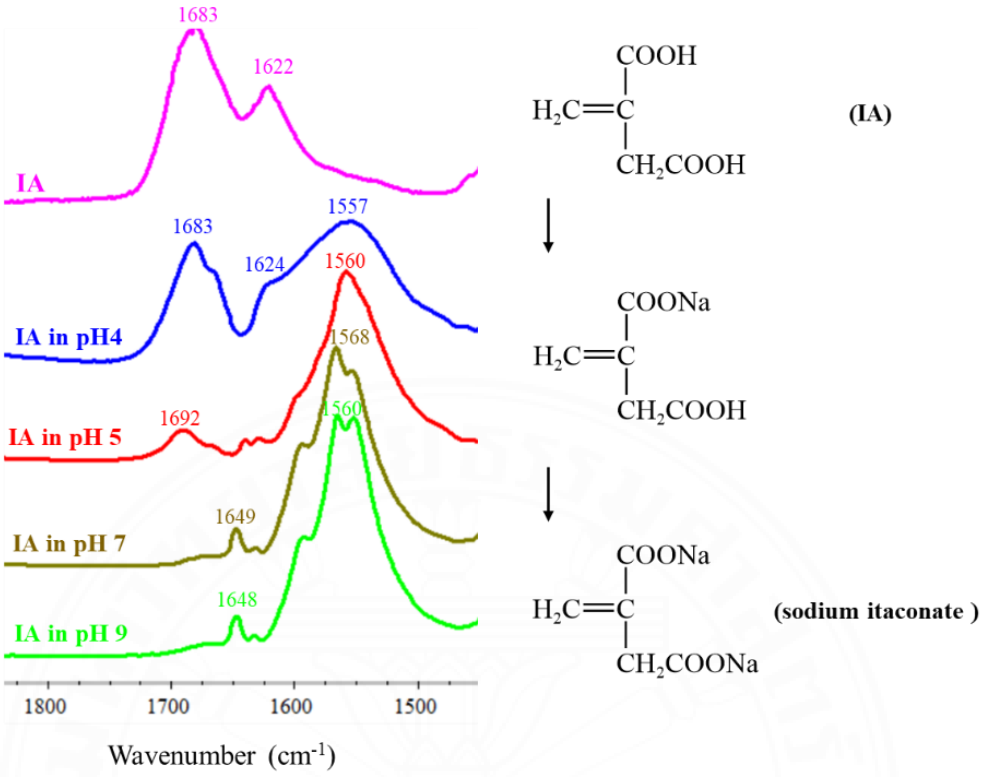

Figure 4.5 FTIR spectra of IA at different pH conditions.

After the neutralization, IA was synthesized to PIA, and the structure of those samples was analyzed by FTIR. FR-PH4 shows numerous COOH groups at peak 1699 cm^{-1}, indicating uncompleted neutralizing of IA structure. While FR-PH7 and FR-PH9 did not show the COOH group around 1700 cm^{-1}. In contrast, FR-PH5, FR-PH7, and FR-PH9 showed strong peaks at 1558 cm^{-1} and 1394 $cm^{-1,}$ corresponding to the asymmetric and symmetric starching of carboxylate group (COO^-), while FR-PH4 showed a lower peak, confirming a lower amount of COO^- (Shi et al., 2017). However, pH 9 shows a lower peak at 1644 cm^{-1} corresponding to C=C, indicating that there are some monomers on FR-PH9 structure. This analysis illustrated the intensity carboxylic acid peak decreased as the neutralization of pH increased. This decrease represents the reduction of the COOH group in the PIA structure, as high pH promotes their deprotonate to carboxylate ions (COO^-). This investigation confirms that the neutralization influences the balance between COOH and COO^- in the PIA structure. However, the optimum synthesis pH for PIA polymerization significantly impacts the polymer structure and applications. Since PIA is used as a biobased antiscalant, the

availability of COO^- is essential to enhance the inhibition performance by increasing scale dispersion (J. Li et al., 2016). Therefore, the synthesis of PIA at pH 9 is selected to continue with another factor. However, the spectrum was similar to another author in a recent publication (Shi et al., 2017).

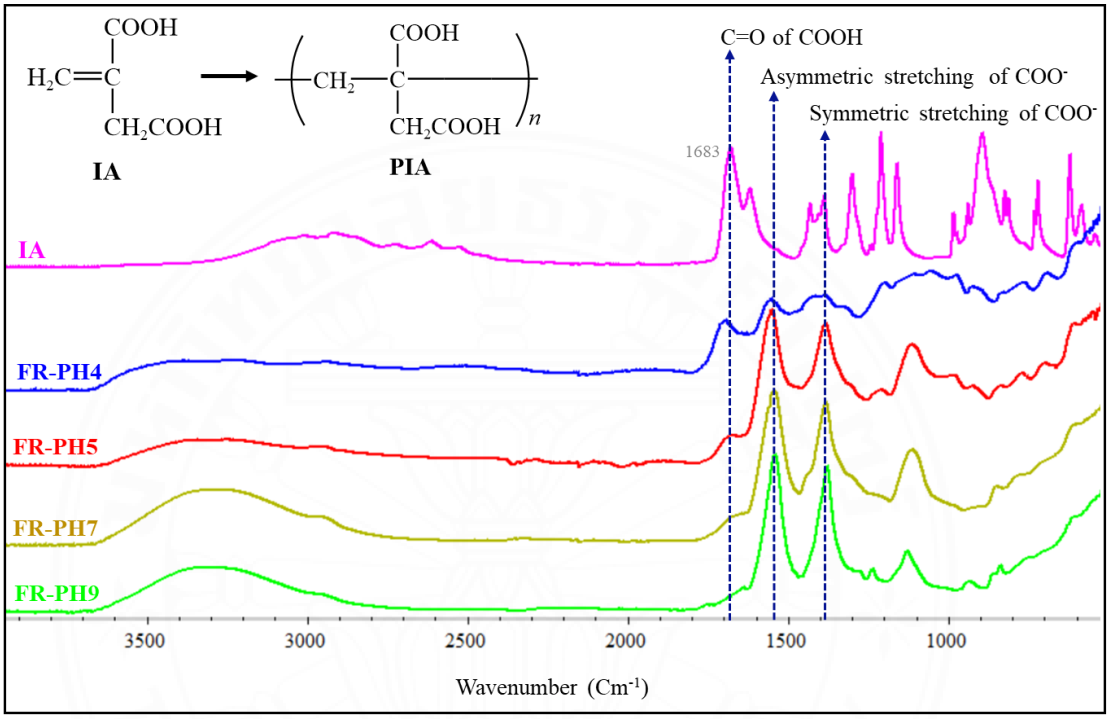

Figure 4.6 FTIR spectra of FR-PH4, FR-PH5, FR-PH7 and FR-PH9

4.2.2 Effect of Initiator concentration

PIA was synthesized by varying the dosage of the initiator. FTIR spectra indicate the effect of the initiator on the polymer chemical structure, as shown in **Figure 4.7**. The structures of PIA were different based on the initiator concentration. Since in this condition, all PIA samples were neutralized to pH 9 before starting the polymerization, PIA exhibit the asymmetric starching of carboxylate ion at ~1548 cm^{-1}, and the symmetric starching of COO^- at ~1385 cm^{-1} (Shi et al., 2017). In addition, a weak peak at~1642 cm^{-1} was observed in FR-A5, FR-A8 and FR-A11, corresponding to double bound (C=C). This means that there are some monomers remaining, while FR-A14 do not illustrate the C=C peak. In this changed structure can be attributed to a high degree of polymerization. The increasing initiator dosage can promote free radicals for initiation and propagation reaction, leading to higher monomer conversion

and increased polymer chain growth (Naghash et al., 2005). These spectra are similar to those reported in a recent publication (Shi et al., 2017).

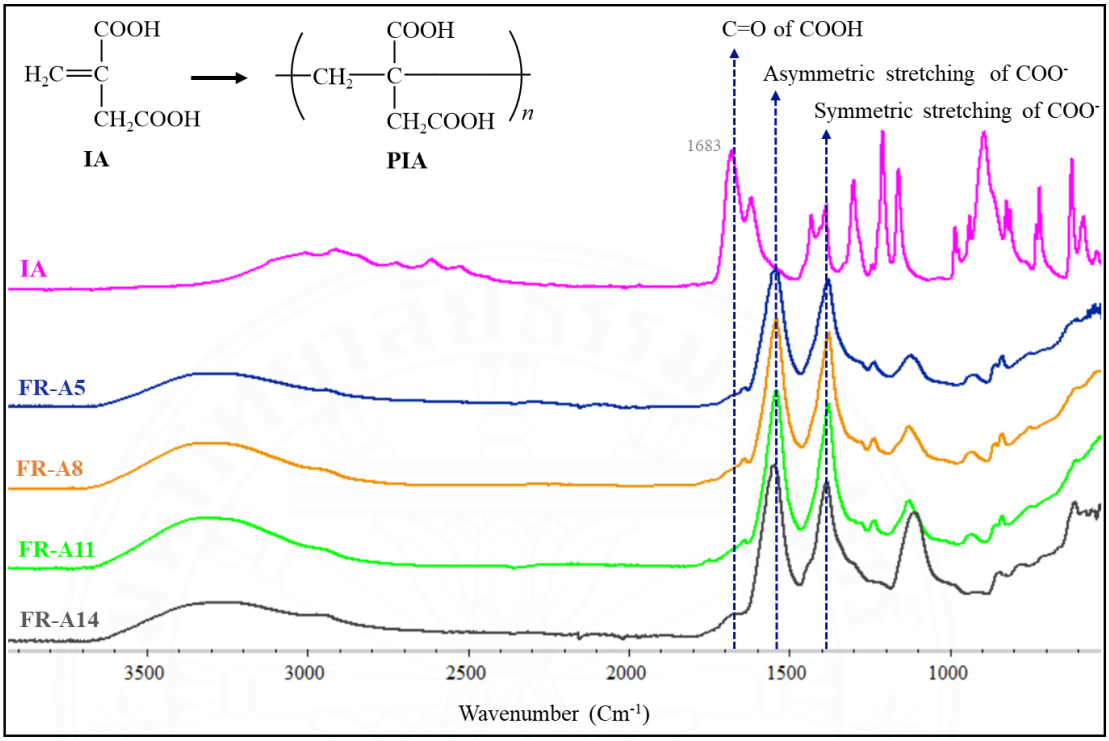

Figure 4.7 FTIR spectra of FR-A5, FR-A8, FR-A11 and FR-A14

4.3 Characterization of PIA by ^{1}H-NMR

4.3.1 Effect of neutralization of IA

The neutralization of IA by NaOH is a critical effect on both structures of IA and PIA. Hence, this discussion will focus on analyzing PIA by ^{1}H-NMR spectra obtained with 600 MHz at 25 °C in D_2O. **Figure 4.8** shows the spectra of products from different pH levels of IA used at the beginning of polymerization. The doublet peak at 5.3 and 5.7 ppm represented the proton in group CH_2= or (a), and the peak around 3.1 ppm represented CH_2- or (b) inside a group of unreacted IA. The strong peak around 4.7 ppm is designated for the solvent D_2O and water.

In addition, the same spectrum also indicated the two broad peaks with similar integration at 2.2 ppm and 2.7 ppm represented to indicate the CH_2- in the backbone (c) and side chain (d). Otherwise, the complete polymerization of IA to PIA of FR-PH4 showed the disappearance of doublet peak (a) of IA, and a peak (b) inside a group of unreacted itaconic acid. Whereas other spectra illustrated (a) peak confirming monomer

remains and incomplete polymerization. In comparison between neutralizing of IA, at pH 4 labeled as FR-PH4 showed the high monomer conversion with disappear of double bone, while FR-PH5 and FR-PH7 have a few monomers remaining and showing as a lower peak of CH_2= and broad peak (c) and (d). While FR-PH9 showed a high intensity of CH_2= peak. However, the lower peaks on the spectrum are caused by the changing the structure of IA during neutralizing due to high temperature (Cao, 2008a). And the structure change of itaconic acid will illustrate in **Figure 4.10**.

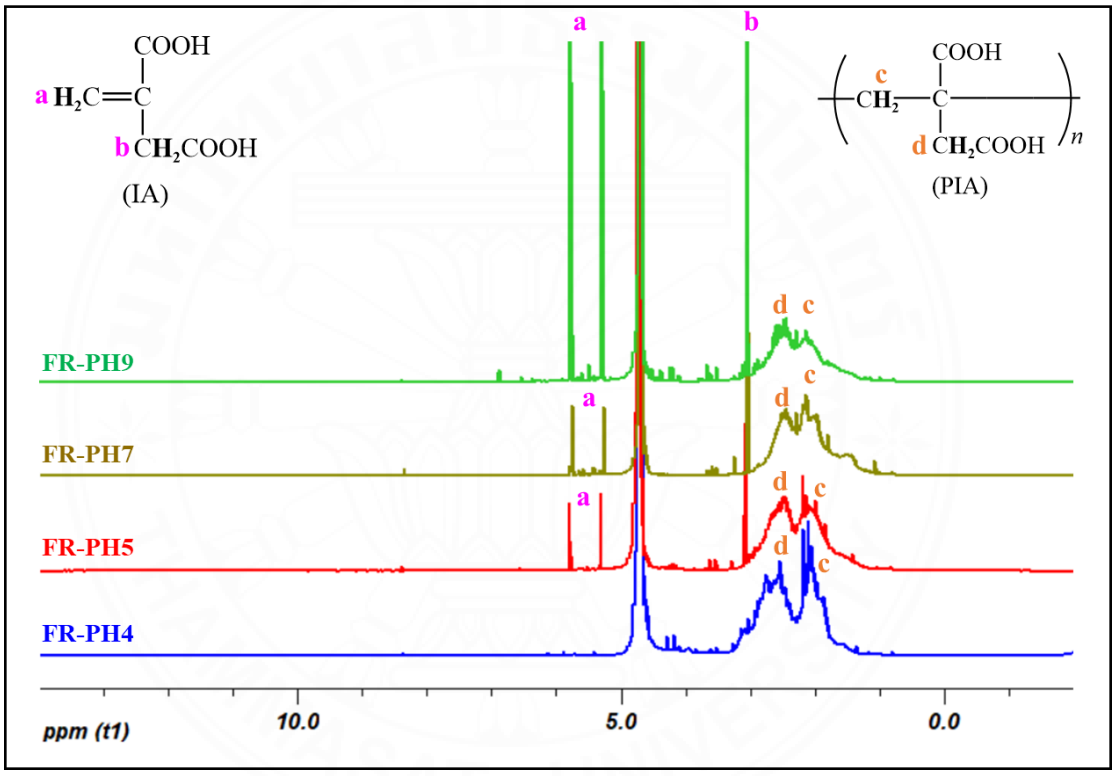

Figure 4.8 ^{1}H-NMR spectra of FR-PH4, FR-PH5, FR-PH7 and FR-PH9

4.3.2 Effect of Initiator concentration

In free radical polymerization, PIA was synthesized using ammonium persulfate (APS) as an initiator. The concentration of the initiator plays an essential role in the polymerization process. **Figure 4.9** shows ^{1}H-NMR spectra of PIA which were synthesized at different initiator concentrations (5%, 8%, 11%, 14%), labeled as FR-A5, FR-A8, FR-A11, and FR-14, respectively. Similar to the previous discussion on neutralizing IA, the four spectra consisted of CH_2= or (a) and CH_2- or (b) inside a group of unreacted itaconic acid. In addition, the same spectra also indicated the two broad

peaks indicated the CH_2- in the backbone (c) and side chain (d). The spectra revealed interesting findings. Specifically, when using a high concentration of APS concentration 14% (FR-A14), the ^{1}H-NMR spectrum displayed a low intensity for CH_2= peak. Additionally, the spectrum exhibited a broadened peak at position (c) and (d). Those observations suggest that the APS concentration could impact the polymerization process potentially influence the degree of polymerization.

Based on those spectra indicated that when the concentration of the initiator is increased, the free radical polymerization of PIA also increases, leading to high monomer conversion (Cao, 2008a; Naghash et al., 2005).

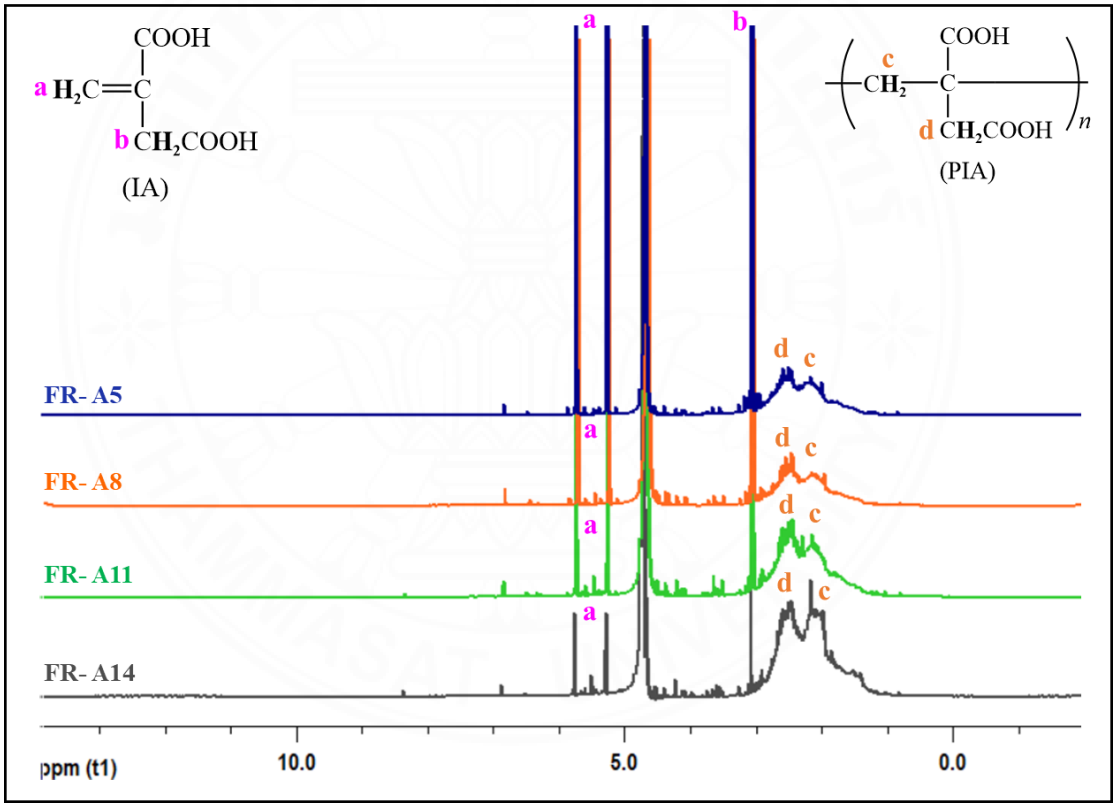

Figure 4.9 ^{1}H-NMR spectra of FR-A5, FR-A8, FR-A11 and FR-A14

The integration (Int.) peak of PIA samples is investigated to obtain the monomer conversion, as illustrated in **Table 4.2**

Table 4.2 The summary of the integration peak of the synthesized samples

Sample code	CH_2= unit		CH_2-	H_p
	Int. a (H_m) (5.7 ppm)	Int. a (5.3 ppm)	Int. (c + d) (2.2-2.7 ppm)	Int. (c + d) / 4
FR-PH4	1.00	0.77	2181.23	545.31
FR-PH5	1.00	1.10	136.12	34.03
FR-PH7	1.00	0.91	91.82	22.96
FR-PH9	1.00	1.03	11.83	2.96
FR-A5	1.00	0.96	6.36	1.59
FR-A8	1.00	0.98	7.03	1.76
FR-A14	1.00	0.98	92.95	23.24

4.3.3 Study the structure modification of PIA during heating.

The major issue of itaconic acid homopolymer is the low molecular weight and monomer conversion as the steric hindrance of IA structure causes the IA to be a sluggish monomer combined with decarboxylation of IA during the free radical polymerization. Therefore, the neutralization step is designed with the aim of overcoming those issues. Once the neutralization is discovered to solve IA polymerization, another challenge occurs as the structure change of IA. In this study, the potential of structural modification based on ^{1}H-NMR of PIA will be investigated in comparison to prior studies. To better comprehend the structure modification of IA was obtained. **Figure 4.10**. summarizes the structure changes of IA when the double bond shifts its position. Based on ^{1}H-NMR spectra, as shown in **Figure 4.8,** at pH 9, FR-pH9 showed peaks at 5.5 and 2.3 ppm. These extra peaks appear when IA was neutralized at high pH (pH 9); at pH 4 and 5, they are almost undetected. The peak at 5.5 and 2.3 ppm correspond to =CH and methyl group (CH_3) of citraconic acid. In contrast, the other two peaks at 2.1 and 6.8 ppm represent CH_3 and =CH of mesaconic acid. This phenomenon is confirmed by a previous study. (Cao, 2008a), in which the authors indicated that at a polymerization temperature 80 ℃, only 1% of citraconic acid and less than 1% of mesaconic acid was formed. However, this structure change is

minimal, which could be neglected, and there is no need to be concerned. In addition, it is common that the synthesized samples can be used without purification.

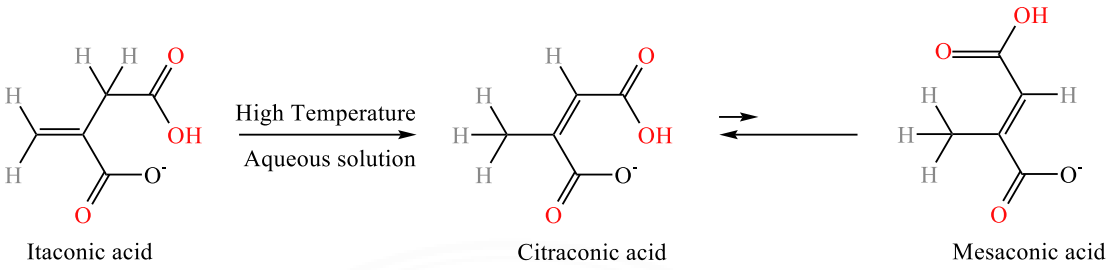

Figure 4.10 Structure changes of itaconic acid to citraconic acid and mesaconic acid

4.4 Monomer conversion and molecular weight of PIA

4.4.1 Effect of neutralization of IA

The effect of neutralizing IA at the beginning of polymerization on monomer conversion and molecular weight of PIA is investigated. As already pointed out, neutralizing helps to eliminate the possibility of decarboxylation stage and enhances the polymerization of IA (Cao, 2008a). Since water is produced during neutralizing IA by NaOH, the concentration of monomer and initiator may slightly alter. However, the high monomer conversion occurs at pH 4 with a monomer conversion of 100 %, while pH 5, 7, and 9 are 97%, 96%, and 75%, respectively. The high polymerization rate led to high molecular weight because the monomer unit reacted to be a longer chain, resulting in high Mw. Hence, when the pH of IA was increased, the Mw slightly decreased.

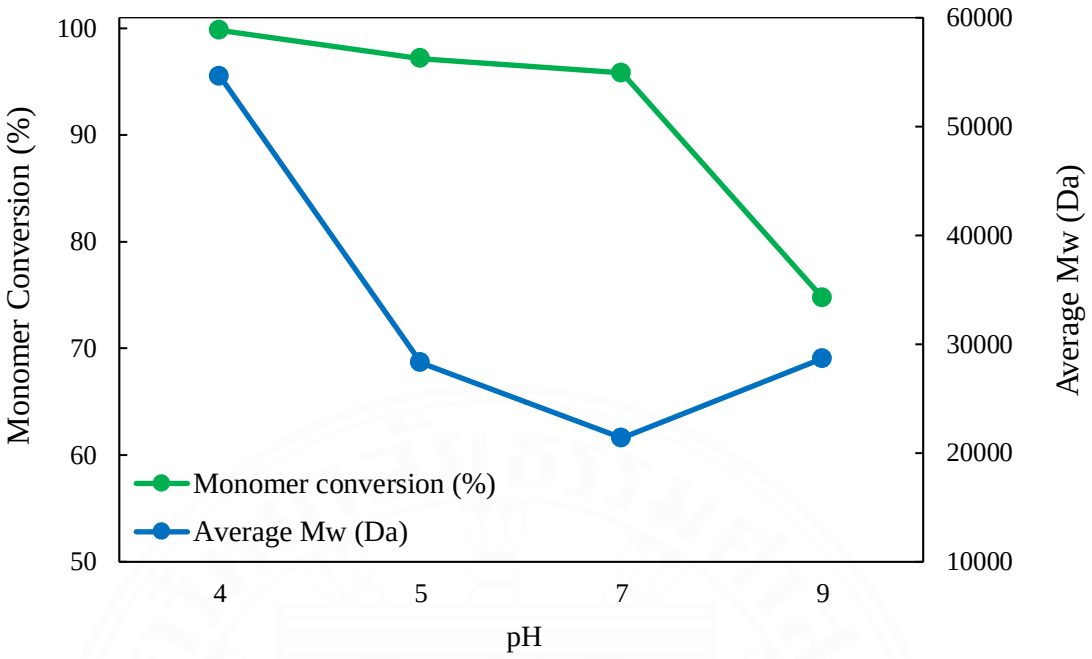

Figure 4.11 The monomer conversion and Mw of PIA by variation of IA's pH

However, the decrease in monomer conversion when the pH increases can be explained by the neutralizing mechanism. IA consists of two carboxylic groups, classified as two acid types (A and B group) based on their respective pKa's. The carboxyl group A, which is next to the double bond, can be stabilized by a conjugative effect and show a lower pKa at 3.85. In contrast, the carboxyl group B has no resonance stabilization, leading to a higher pKa at 5.45 (Cao, 2008b). During the neutralization step, group A was dissociated first, as shown in **Figure 4.12a.** In addition, the neutralizing of acid group A at pH 4 could increase the stability of free radicals when IA monomer was attacked by the initiator, as illustrated in **Figure 4.12b.** Once the neutralizing is exceeded, the monomer conversion decreases because when both acid groups A and B are neutralized, they will generate numerous ionic (negative charge), and it might cause ionic repulsion. Then, it decreased initiator efficiency, ammonium persulfate (negative charge), resulting in decreased polymerization rate.

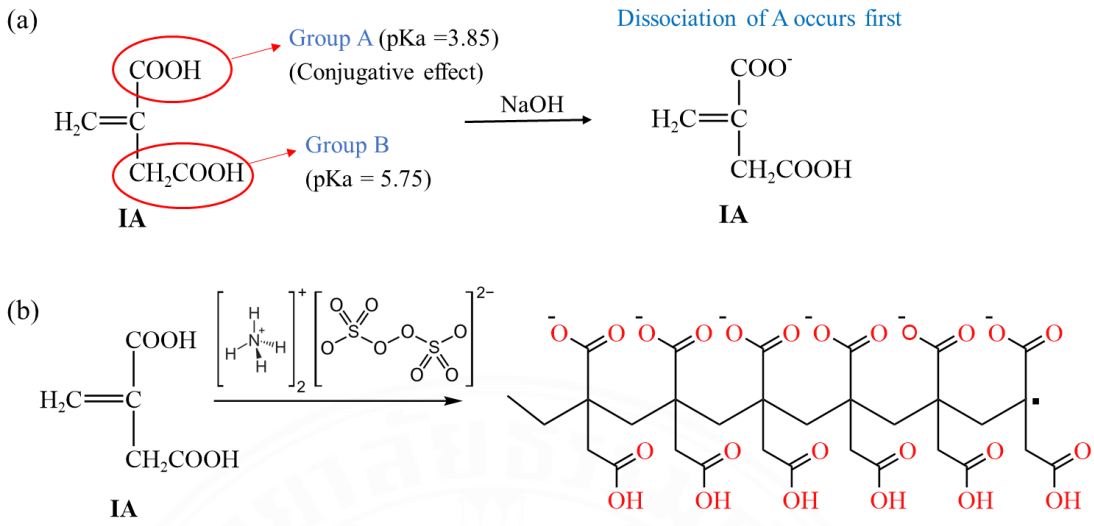

Figure 4.12 a). The partial neutralization of IA. b). The reaction equation of PIA by half neutralization at pH 4 (Cao, 2008b).

4.4.2 Effect of Initiator concentration

The effect of initiator (APS) concentration on monomer conversion and molecular weight of PIA from free radical polymerization is summarized in **Figure 4.13**. APS in the polymerization of IA has a significant effect on monomer conversion. Increasing APS concentration results in enhanced radical production, which could accelerate the polymerization rate, and improve monomer conversion. This scenario can explain that APS (14%) has high monomer conversion (96%) because higher APS concentration could accelerate the generation of free radicals for propagation. In consequence, a high amount of APS leads to a higher monomer conversion (Cummings et al., 2016). However, the minimal APS concentration (5%) illustrated a poor monomer conversion because a small amount of APS might slowly create free radicals, resulting in sluggish propagation in the polymerization stage (Cao, 2008a).

In contrast, the concentration of the initiator also affects Mw of the polymers. The results showed that the average Mw of FR-A5 is 31117 Da, while the average Mw of FR-A8 is 32206 Da. The slight increase of Mw is likely because the increase of initiator could promote the monomer conversion by quick propagation. This leads to longer polymer chains and higher molecule weight. While the average Mw of FR-11 and FR-A14 is 28672 Da and 19675 Da, respectively. The decrease of Mw when APS

increases is because the exceeded initiator concentration will boost the termination rate, resulting in a lower Mw (Okada et al., 2021). Therefore, to maintain the required Mw, that is critical to consider the initiator concentration.

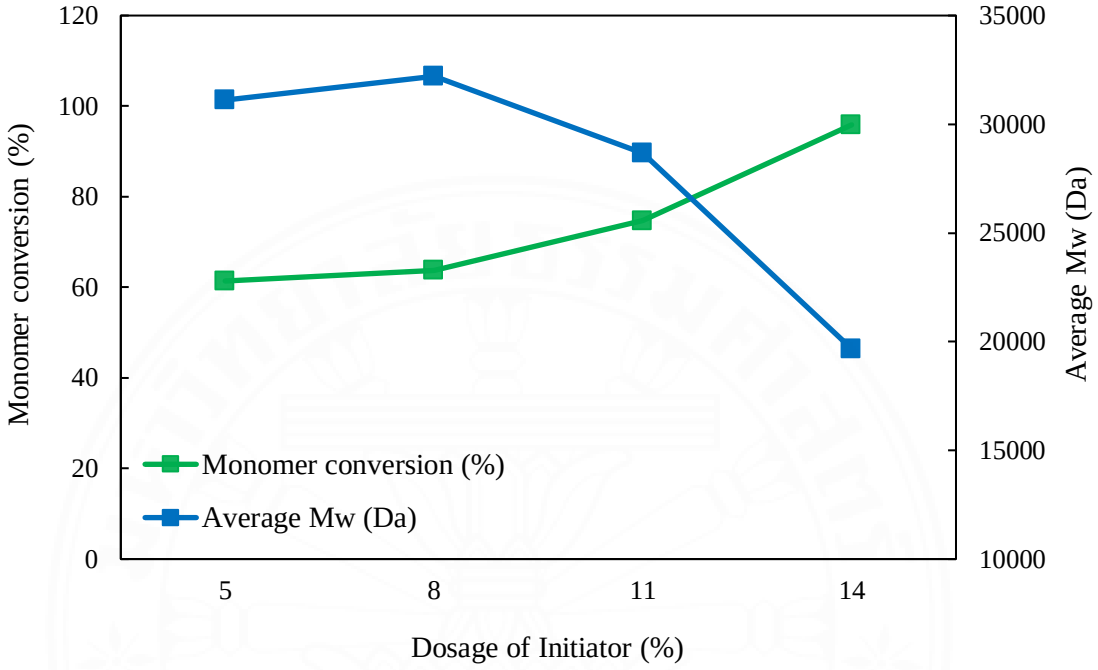

Figure 4.13 The monomer conversion and Mw of PIA by variation of initiator concentrations.

4.4.3 Effect of Initiator on pH of PIA

To understand the pH change during polymerization from **Table 4.3**, it is essential to understand the reaction of the initiator (APS) and the mechanism of APS first. The reaction mechanism of APS is (House, 1962; van Berkel et al., 2006):

$$(NH_4)_2S_2O_8 \rightarrow 2(NH_4)^+ + S_2O_8^{2-} \quad (1)$$

$$S_2O_8^{2-} \rightarrow 2SO_4^{-\bullet} \quad (2)$$

$$2SO_4^{-\bullet} + H_2O \rightarrow HSO_4^- + OH^\bullet \quad (3)$$

$$2OH^\bullet \rightarrow H_2O + 1/2\ O_2 \quad (4)$$

- The proposed mechanism of pH increased for neutralizing IA in weak acids (pH 4, pH 5) is getting by the hydrolysis of ammonium ion $(NH_4)^+$:

  $(NH_4)^+ + H_2O \rightleftharpoons NH_3 + H_3O^+$

Furthermore, the generation of water equation (4) could promote the increase of pH.

- The proposed mechanism of pH decreases after neutralizing of IA in weak based (pH 9) is getting by $SO_4^{\bullet-}$ reaction with protons (H^+) producing HSO_4^- which are acidic in nature.

  $2SO4^{\bullet-} + 2H^+ \rightarrow 2\ HSO_4^-$

In addition, the generation of (HSO_4^-) in equation (3) might help lower the pH of PIA (Bednarz et al., 2015).

Table 4.3 Summary of Mw, monomer conversion, and pH of PIA synthesized by free radical polymerization.

Sample	**Average Mw** (Daltons)	**Monomer Conversion** (%)	**pH of the sample**
FR-PH4	54633	100	4.5
FR-PH5	28285	97	5.97
FR-PH7	21380	96	7.53
FR-PH9	28672	75	6.83
FR-A5	31117	61	6.99
FR-A8	32207	64	6.75
FR-A14	19675	96	7.46

4.5 Antiscalant Performance of PIA on $CaCO_3$

4.5.1 Effect of pH of IA

The effect of the pH of IA before the polymerization on scale inhibition performance of the resulting PIA is investigated by varying the concentration of PIA from 20 mg/L to 100 mg/L. The results, as shown in **Figure 4.14** indicate that FR-PH9 has the highest scale inhibition efficiency, around 87 %, at a dosage of 40 mg/L. While at the same dosage, FR-PH7, FR-PH5, and FR-PH4 show only 79, 50, and 11 %, respectively. When the antiscalant concentration was increased from 20 to 100 mg/L, the inhibition efficiency of FR-PH9 and FR-PH7 increased slightly, while FR-PH4 increased four times and FR-PH5 increased 2 times. The slight increase in FR-PH9

performance indicated their effectiveness even at low concentrations, and it might already reach the optimum inhibition percentage.

The antiscalant performance depends on the pH of IA, which is neutralized by NaOH at the beginning of the free radical polymerization process. The higher pH indicated a high concentration of COO^-, whereas the low pH indicated a minimal concentration of COO^-. PIA synthesized at pH 9 (FR-PH9) facilitates greater electrostatic interaction between negative charges of PIA molecules with scale Ca^{2+}. Those interactions promote PIA adsorption on scale-forming surfaces and limit scale formation. In order words, the carboxylate ion generated during neutralization can be used against scale formation (Zhao et al., 2021). The COO^- has the potential to suppress scale formation because they are negative charges, and they could prevent Ca^{2+} from forming scale formation ($CaCO_3$). The numerous numbers of negative charges on the PIA structure could cause ion repulsion by repelling the negative charge of CO_3^{2-} away from Ca^{2+}. This helps to reduce the possibility of scale formation (J. Li et al., 2016). Moreover, the carboxylate groups in PIA act as active sites for binding with scale-forming ions (Ca^{2+}). The concentration of carboxylate ions increases with increasing pH, resulting in greater availability of active sites for interaction with Ca^{2+} (Zhao et al., 2021). The greater carboxylate ion concentration of FR-PH9 contributes to better scale inhibition efficacy than other PIA from low pH.

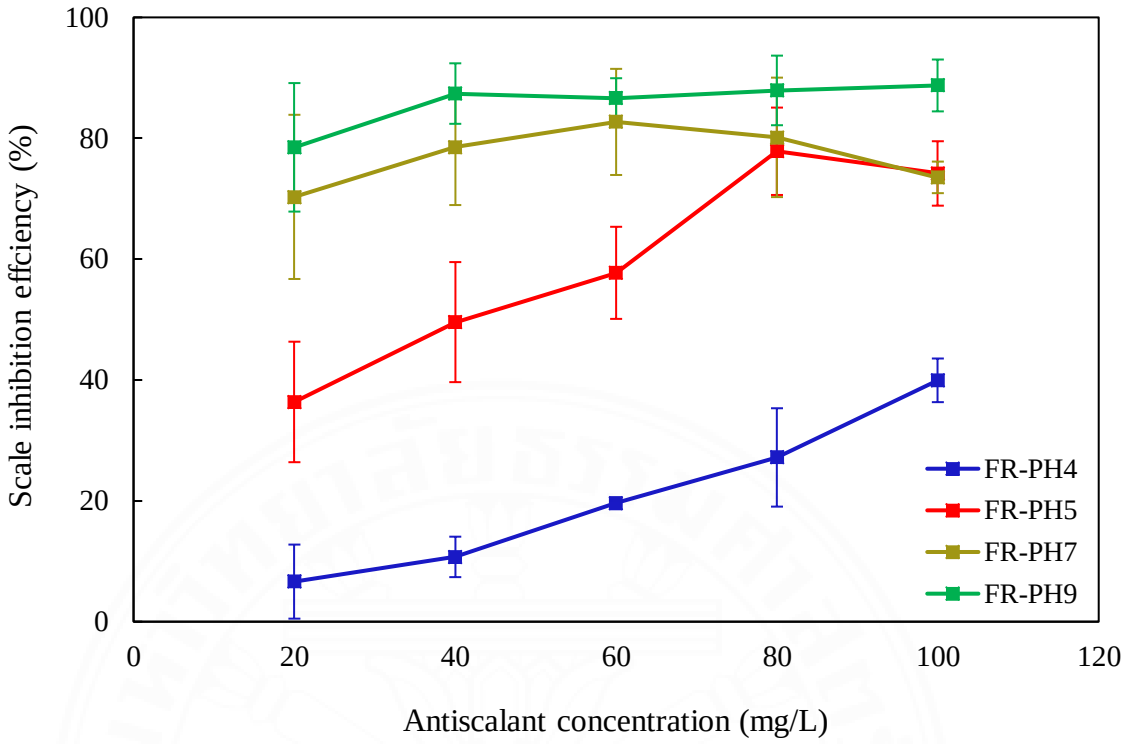

Figure 4.14 Antiscalant performance of FR-PH4, FR-PH5, FR-PH7 and FR-PH9

4.5.2 Effect of initiator concentration

The impact of initiator concentrations on antiscalant efficiency was evaluated against calcium carbonate. The scale inhibition efficiency of FR-A5, FR-A8, FR-A11, and FR-A14 are summarized in **Figure 4.15.** The results demonstrated that the inhibition percentage increased with rising PIA concentration. Once the dosage of PIA reached an excess level, the inhibition efficiency remained stable. FR-A11 or FR-PH9 is the same condition, which demonstrated the highest efficiency compared with another condition of initiator concentration. From a dosage of 20 to 100 mg/L, the antiscalant performance of FR-A5 and FR-A8 increased almost three times, while FR-A14 enhanced around 2 times. However, the variety of initiators aims to maintain the molecular weight of PIA, and it also impacts the conversion rate. Therefore, to understand the impact of scale inhibition performance, we should understand the molecular weight and monomer conversion of those materials first. **Table 4.3** summarizes the average Mw of PIA. The results show a decreasing trend, as follows: FR-A8 > FR-A5 > FR-A11 > FR-A14, while the monomer conversion of PIA increased, as follows: FR-A5 < FR-A8 < FR-A11 < FR-A14. The high inhibition

performance of FR-A11 (Mw = 28 672 Da) might be due to the optimum molecular weight, which is quite close to the optimum Mw (Mw = 24 100 Da) of a previous report (Yang et al., 2017). Once FR-A5 (Mw = 31 117 Da) and FR-A8 (Mw = 32 207 Da) have a higher Mw than FR-A11, their antiscalant performance is not over FR-A11 as the high molecular weight might not be effective on Ca^{2+} due to the bulky molecule. In contrast, FR-A14 (Mw = 19 675 Da) is also effective on scale inhibition, but its performance is still lower than FR-A11 because it has a low Mw. The low molecular weight limits the binding capacity of carboxylate and calcium. These findings indicate that the Mw has a significant effect on the scale inhibition efficiency. An optimum molecular weight for PIA in this study is around 20 000 Da – 30 000 Da.

It is crucial to note that in terms of scale inhibition efficacy, PIA should have a suitable Mw range. The optimum Mw provides a greater functional group for enhanced absorption and inhibition of scale crystal nucleation. Extremely high molecular weights may cause steric hindrance and be unsatisfactory for Ca^{2+}, while extremely low molecular weights can result in insufficient coverage and limited inhibition ability. It is critical to optimize the scale inhibition efficacy of PIA by balancing its molecular weight (Yang et al., 2017).

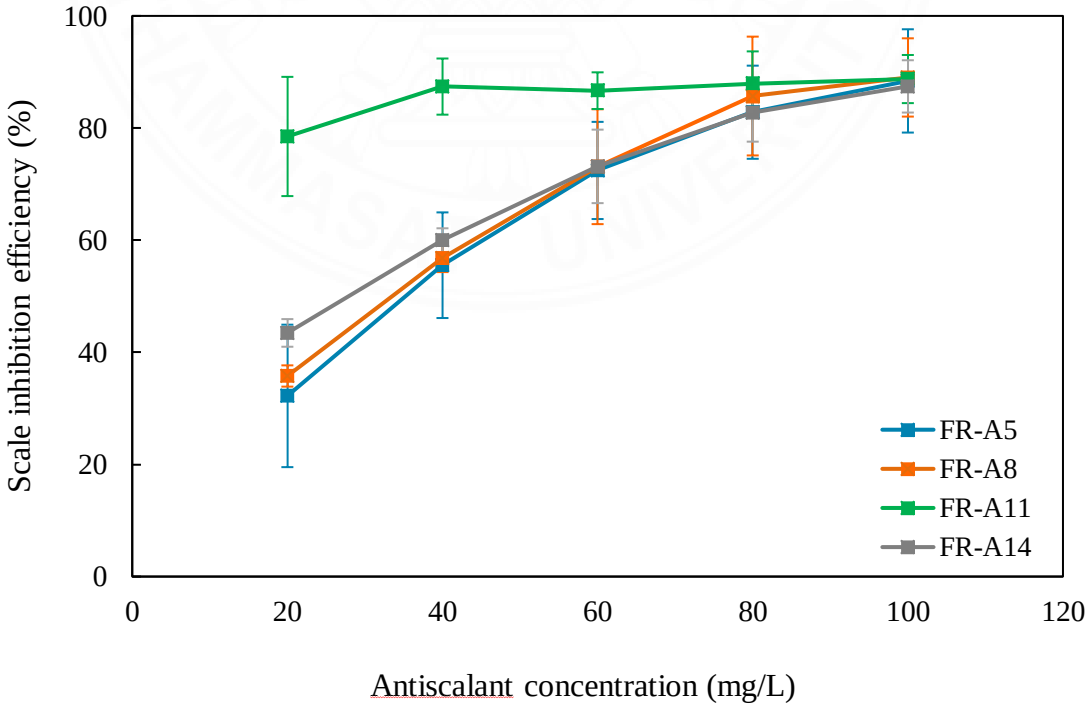

Figure 4.15 Antiscalant performance of FR-A5, FR-A8, FR-A11, and FR-A14

Importantly, based on the observation during the antiscalant's efficiency tests, only FR-PH7 and FR-PH14 clearly showed sediment on the bottom of the test tube at a dosage of 100 mg/L, while the rest of PIA samples showed undetected precipitation. This might be the reason why the scale inhibition of both FR-PH7 and FR-A14 is not more effective when they were applied in high concentration.

4.6 The re-neutralizing of FR-PH4 and FR-PH5

Two samples are synthesized in weak acid form, i.e., FR-PH 4 and FR-PH 5, which were synthesized by neutralizing IA at pH 4 and 5, respectively. Due to the lack of COO^- on both structures, the antiscalant performance was poor. To enhance the deprotonation of COOH group, both samples were neutralized with NaOH to pH 7 and pH 8 in polymeric form. FTIR results illustrate that the remaining COOH were further deprotonated, leading to strong COO^- peak at 1560 cm^{-1} and 1380 cm^{-1}, as shown in **Figure 4.16 .** The amount of carboxylate ion improved when FR-PH4 was neutralized to pH 7 and pH 8, and the efficacy of scale inhibition was slightly increased from 11 to 38 and 40%, respectively. The high Mw of the materials, which is not effective for $CaCO_3$ inhibition, causes an increased somewhat scale inhibition. Similarly, the scale inhibition percentage of FR-PH5 slightly increased after being neutralized to pH 7 and pH 8, as illustrated in **Figure 4.17**.

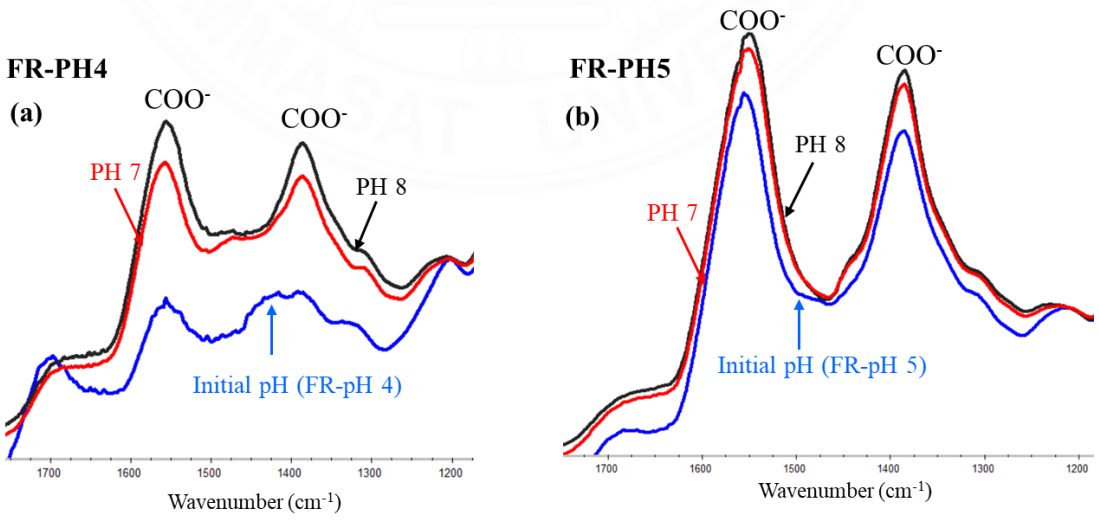

Figure 4.16 FTIR spectra of a) FR-PH4 and b) FR-PH5 before and after neutralizing at pH 7 and 8.

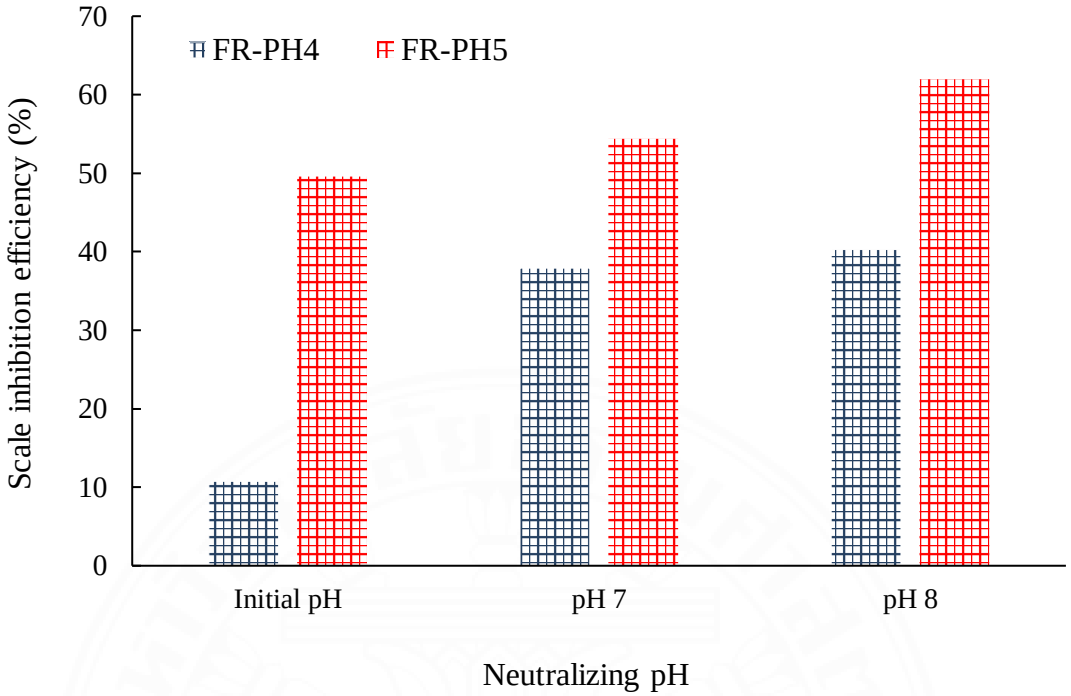

Figure 4.17 The antiscalant performance of original FR-PH4 and FR-PH5 and those after neutralization, at a dosage of 40 mg/L.

4.7 The factors that affect PIA performance.

Since FR-PH9 illustrated the highest scale inhibition performance, this material was selected to study the factor effect on scale inhibition performance, including effect of antiscalant concentration, concentration of Ca^{2+} and HCO_3^-, pH of water, and heating time.

4.7.1 Effect of PIA concentration

The impact of antiscalant concentration on the inhibition against calcium carbonate scale deposit was evaluated at 5 to 25 mg/L. The measurements were conducted at the initial pH of distilled water. The result is shown in **Figure 4.18**. The inhibition efficiency is increased based on the concentration of the antiscalant. At a dosage of 5 mg/L, the inhibition percentage is 50 %. While at a dosage of 10 mg/L, the inhibition percentage reached 81 and 93 % at 20 mg/L. When the antiscalant concentration is in excess, the inhibition is not further increased. This indicates that the scale inhibition efficiency improves with the PIA concentration or the carboxylate ion

content. However, once the antiscalant reaches a certain level, the scale inhibition performance is stable (Y. Liu et al., 2014; Tang et al., 2017).

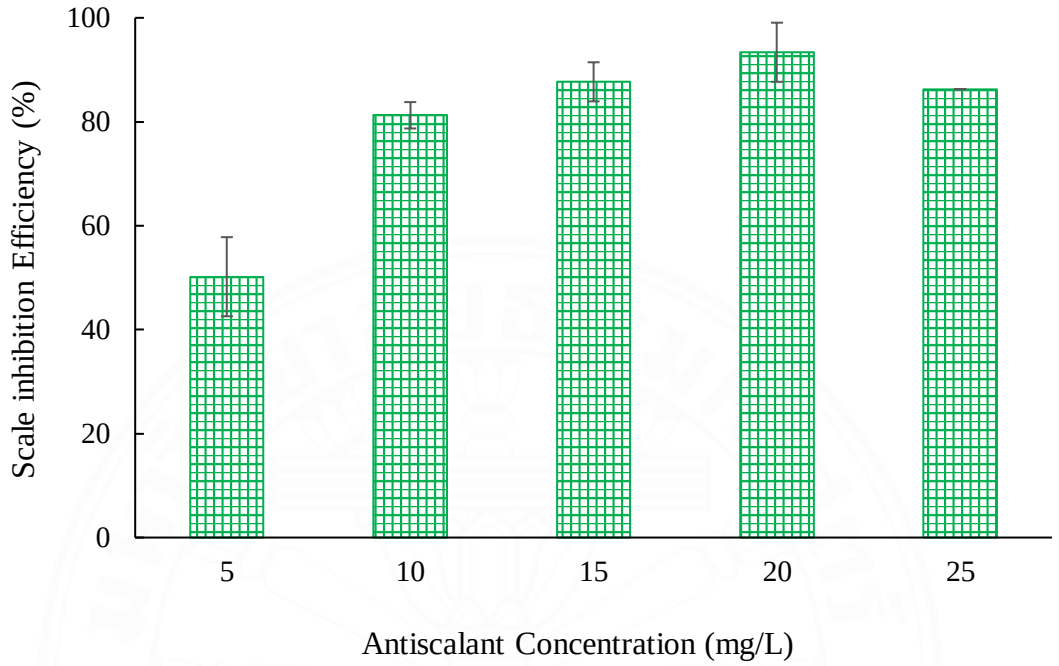

Figure 4.18 Effect of FR-PH9 concentration on antiscalant performance.

4.7.2 Effect of concentration of Ca^{2+} and HCO_3^-

Generally, the content of calcium ions depends on the type of water. A typical freshwater calcium level ranges from 4-100 mg/L, while eutrophic water and seawater contain calcium higher than 25 mg/L and 400 mg/L, respectively (Calcium and Water Hardness, 2011). To determine the tolerance concentration of calcium and bicarbonate, PIA was employed at 40 mg/L. The study ratio of Ca^{2+} and HCO_3^- are 250 mg/L, 500 mg/L, 750 mg/L and 1000 mg/L. As shown in **Figure 4.19**, the concentration of Ca^{2+} and HCO_3^- significantly influences the antiscalant performance. When the concentration of Ca^{2+} and HCO_3^- was 250 mg/L, the efficiency of PIA was 89 % and sharply decreased to 29 % when the concentration increased to 1000 mg/L. Based on the result, the antiscalant performance percentage is reduced by increasing the concentration of Ca^{2+} and HCO_3^- (Xiao et al., 2022). The decrease in scale inhibition performance was because the amount of PIA was stable at a dosage of 40 mg/L, limiting the capability of functional groups to capture the free calcium ion. Additionally, when the concentrations of Ca^{2+} and HCO_3^- increased, calcium carbonate was raised and

reduced the scale inhibition performance (Huang et al., 2019). Eventually, the PIA might not be tolerant to high calcium concentrations, but they still perform well at 250 mg/L. This confirms that PIA is effective in water facility applications, which is especially suitable for reverse osmosis processes.

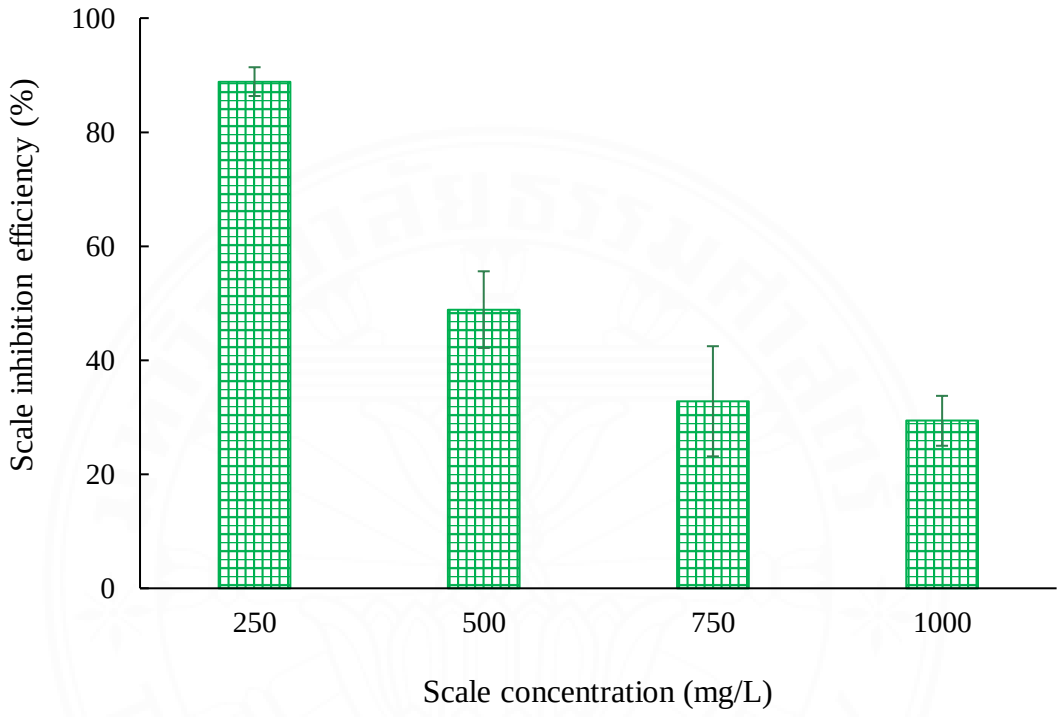

Figure 4.19 Effect of scale concentration on antiscalant performance.

4.7.3 Effect of pH of the water

Since the pH of water in general circulating water facilities are commonly neutral or slightly alkaline, the scale inhibition efficiency of PIA was evaluated in solution with pH from 6 to 10, as shown in **Figure 4.20**. At pH 6, the efficiency of scale inhibition of PIA is low compared to at pH 7 and 8 because some carboxylic groups might not deprotonate to be COO^-, which reduces the scale inhibition capability. At pH 7-8, the scale inhibition percentage rapidly increased as all carboxyl groups were deprotonated. When the pH was further increased, however, the antiscalant performance significantly decreased from 95 % at pH 8 to 63 % at pH 9. This is likely because, at this high pH, the large amount of hydroxyl groups may interact with bicarbonate, increasing the number of carbonate ions, which is the origin of the calcium carbonate scale. Also, the hydroxyl groups have a stronger chelating capacity than the

carboxylate groups, which might interact with free calcium ions. Additionally, the higher pH is also beneficial for calcium carbonate growth since the solubility of calcium carbonate is rapidly decreased at high pH (Luo et al., 2015).

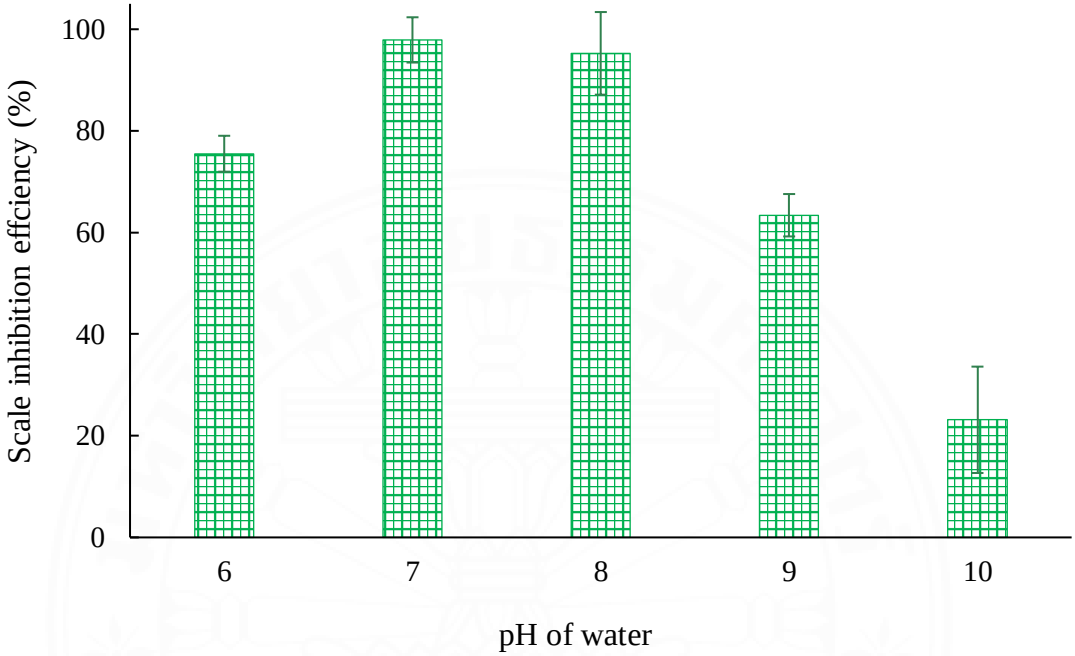

Figure 4.20 Effect of pH of water on antiscalant performance

4.7.4 Effect of heating time

Heating time is another important factor in antiscalant performance. **Figure 4.21** illustrates the effect of heating time (12, 24, 48, and 72 h) on the inhibition efficiency at an initial pH of PIA and a dosage of 40 mg/L. The results indicate that the antiscalant against calcium carbonate is effective at 10 and 12 h with an inhibition percentage of 87 and 75 %, respectively. This dramatically declined to 51 % at a heating time of 24 h, and further decreased to 44 % at 72 h. This is likely because PIA partially binds with calcium ions and precipitates, leading to a lower content of effective PIA in the water system. To overcome this, continuous antiscalant injecting should be applied to enhance the scale inhibition percentage (Luo et al., 2015).

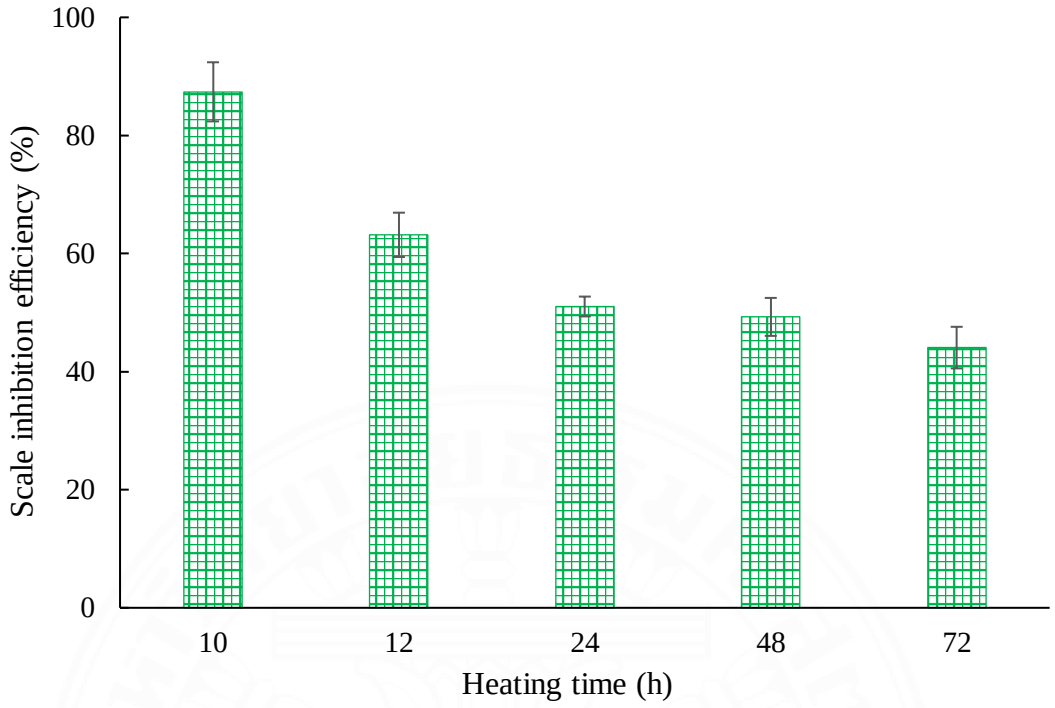

Figure 4.21 Effect of heating time on antiscalant performance.

4.8 Study the morphology and mechanism of PIA performance on $CaCO_3$

The crystal morphology of $CaCO_3$ was analyzed using scanning electron microscopy (SEM) to investigate the impact of PIA on crystal morphology and the antiscalant mechanism. The observation of morphology was compared between the $CaCO_3$ scale deposit without antiscalant compared with the $CaCO_3$ scale deposit under the presence of FR-PH9 at a dosage of 10 mg/L, as summarized in **Figure 4.22**. Generally, the morphology of $CaCO_3$ in the absence of an antiscalant is higher than in the presence of an antiscalant. In this phenomenon, the $CaCO_3$ in the absence of FR-PH9 shows more regular aragonite crystallization. When FR-PH9 was added to the treatment sample, the amount of scale dramatically declined, indicating that FR-PH9 has a better-dispersing property, reducing the collision frequency of $CaCO_3$ crystal growth and keeping the scale in the microcrystal stage (Shi et al., 2017). In this phenomenon, the mechanism of FR-PH9 is stabilizing particle dispersion due to the numerous amounts of COO^- creating repulsive barriers with the negative charge of CO_3^{2-} and keeping the particle dispersed in solution.

In contrast, the crystal form of $CaCO_3$ scale changes to an irregular shape (sphere shape), making the crystal structure less appearance and blocking the crystal

growth (Du et al., 2018). This scenario illustrates that the FR-PH9 could inhibit the growth of the active site of $CaCO_3$, and they could interact with the crystal surface and cause crystal lattice distortion (Du et al., 2018). However, this indicates that another mechanism of FR-PH9 with $CaCO_3$ is crystal modification.

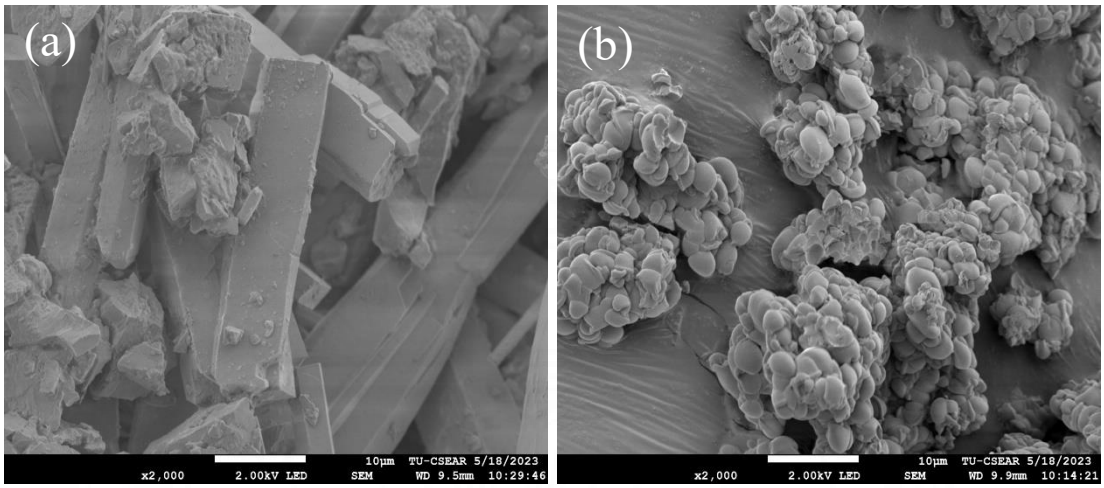

Figure 4.22 The morphology of $CaCO_3$ recorded by SEM. a) without antiscalant. b) with the presence of 10 mg/L of FR-PH9.

4.9 Comparison of PIA performance with commercial antiscalants

The performance of PIA was evaluated and compared with the commercial antiscalant, which developed from polymaleic acid (PMA), 2-Phosphonobutane-1,2,4-tricarboxylic acid (PBTC), and the monomer of itaconic acid (IA) as mentioned in **Figure 4.23.** The pH of those commercials antiscalant is 0.3 for PMA, and 0.2 for PBTC. The treatment test was evaluated at 20 mg/L in the initial pH of the water**.** The antiscalant performance of FR-PH9 was promoted to 79 %. In contrast, IA, PMA, and PBTC could inhibit $CaCO_3$ only 11, 61, and 65%, respectively. The results illustrate that FR-PH9 showed a better inhibition than the existing commercial antiscalant. More importantly, the better inhibition efficiency of PIA over the commercial antiscalants is likely because of its higher number of COO^-, which is more hydrophilic and makes the $CaCO_3$ more disperse in the water. While based on the observations, during antiscalant treatment, the binding of PMA and Ca^{2+} causes sediment, and it might be reduced the PMA content, leading to a lower free Ca^{2+} after treatment. However, based on a previous report, the pKa of PMA is around 5 to 7 (Mohanty et al., 2013), while the pKa

of three carboxylic groups on PBTC structure is 3.92, 4.76 and 6.13 (Jerome et al., 2022). The lower pH of PMA and PBTC solutions led them to carboxylic group form, while when it was applied in the treatment test (pH = 7.5~8.0), they will deprotonate and bind with Ca^{2+}. However, there might be more competition with CO_3^{2+}, limiting their abilities. Hence, the presence of COO^- on the PIA structure could enhance the scale inhibition efficiency.

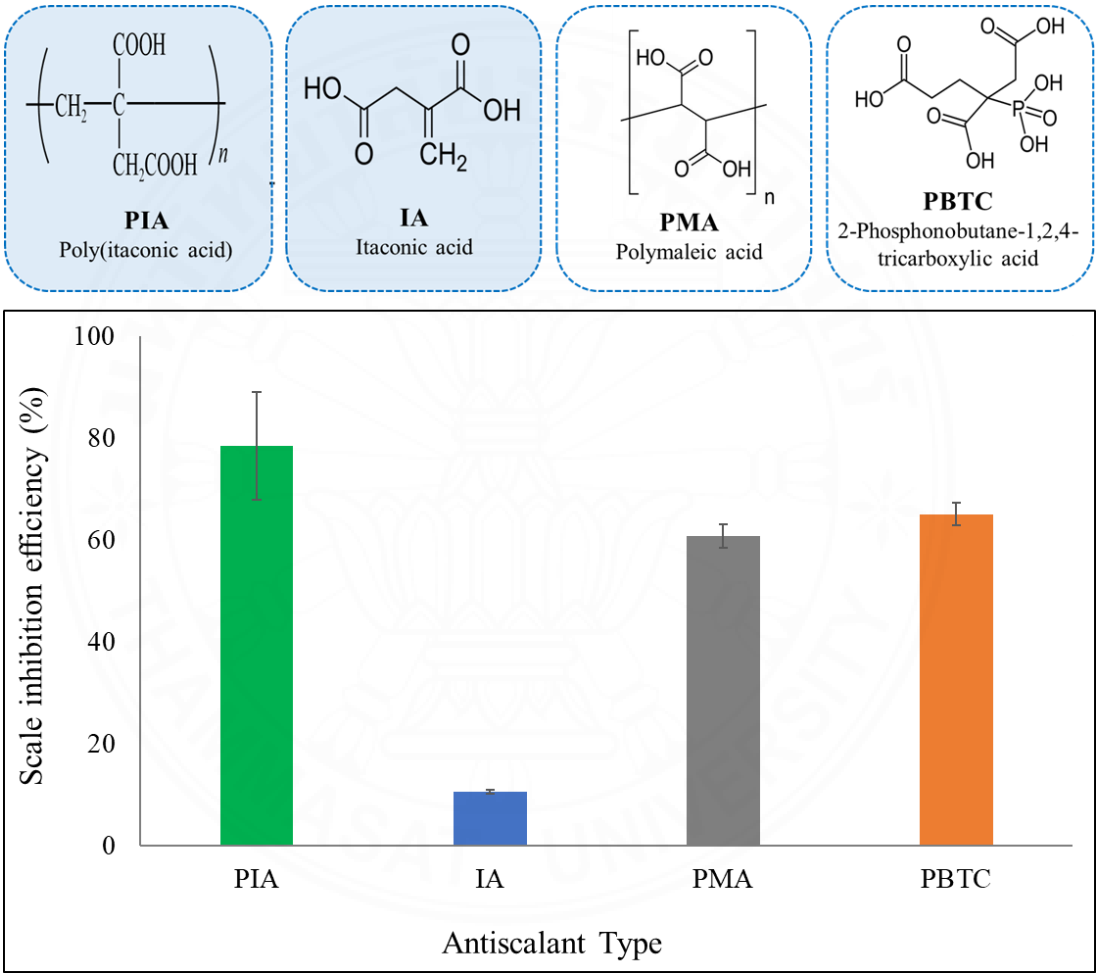

Figure 4.23 The comparison of PIA and commercial antiscalant performance at initial pH and their chemical structure.

CHAPTER 5
CONCLUSIONS

Poly(itaconic acid) has been synthesized using various techniques, including emulsion polymerization (EP-N30), phase inversion emulsification (PI-N30), and free radical polymerization (FR-). The materials were successfully characterized by FTIR, GPC, and ^{1}H-NMR spectroscopy. The materials are intended for applications in scale inhibition. The findings demonstrated that:

(a). The highest monomer conversion is achieved in free radical polymerization under 85 ℃ for 4 h conditions.

(b). In free radical polymerization, neutralizing IA to pH 4 before the polymerization results in the maximum monomer conversion (100%). In addition, neutralizing IA before polymerization is also critical in suppressing decarboxylation during the polymerization.

(c). FTIR spectra of FR-A5, FR-A8, FR-A11, FR-A14, FR-PH5 and FR-PH7 illustrated the numerous carboxylate ions on their chemical structures. While FR-PH4 demonstrated lower deprotonation of COOH.

(d). The pH of IA has a significant impact on PIA structures. Neutralizing IA at lower pH before polymerization helps to enhance the stability of radicals. If IA is excessively neutralized, it will cause ion repulsion and decrease the monomer conversion. Based on the effect of pH of IA, the monomer conversion is reduced, as follows: FR-PH4 > FR-PH5 > FR-PH7 > FR-PH9.

(e). Initiator concentration is another factor impacting the PIA structure. When the initiator concentration is increased, numerous free radicals occur, resulting in a rise in the monomer conversion. The monomer conversion rate has risen, as follows: FR-A5 < FR-A8 < FR-A11< FR-A14.

(f). The neutralization impacts not only the monomer conversion but also antiscalant effectiveness. Neutralizing IA at higher pH will improve the deprotonation of COOH to numerous COO^{-} leading to great efficacy in inhibition performance.

(g). To maximize the scale inhibition efficiency of PIA, the molecular weight of PIA should be controlled to an appropriate level. High Mw might deliver many active

groups, preventing scale expansion. However, if the Mw is too high, steric hindrance will occur, resulting in diminished scale inhibition.

(h). Neutralizing PIA after synthesis enhanced additional deprotonation of residual COOH and slightly increased inhibition performance.

(i). Many factors affect antiscalant performance, including the concentration of antiscalant, concentration of scale, pH of water, heating time, and molecular weight of the polymer.

(j). The main mechanism of PIA on $CaCO_3$ is stabilizing particle dispersion, which gets from the presence of COO^- in the PIA structure, and crystal modification which forms an irregular crystal growth of $CaCO_3$.

(k). The synthesized PIA performs similarly to commercial antiscalants, such as PBTC and PMA. However, the environmentally friendly bio-based PIA has a high potential for practical applications as it performs similarly to other commercial antiscalants.

REFERENCES

Abdel-Aziz, H. M. (2011). Template preparation of poly(vinylpyrrolidone-itaconic acid) and their application in removal of copper ions. *Polymer - Plastics Technology and Engineering*, *50*(10), 1011–1018. https://doi.org/10.1080/03602559.2011.553873

Al Omari, M. M. H., Rashid, I. S., Qinna, N. A., Jaber, A. M., & Badwan, A. A. (2016). Calcium Carbonate. In *Profiles of Drug Substances, Excipients and Related Methodology* (1st ed., Vol. 41). Elsevier Inc. https://doi.org/10.1016/bs.podrm.2015.11.003

Amjad, Z., & Koutsoukos, P. G. (2014). Evaluation of maleic acid based polymers as scale inhibitors and dispersants for industrial water applications. *Desalination*, *335*(1), 55–63. https://doi.org/10.1016/j.desal.2013.12.012

Asif.A, M., & Kaneko, T. (2017). Microbe-Derived Itaconic Acid: Novel Route to Biopolyamides. *Microbial Applications*, *2*, 1–336. https://doi.org/10.1007/978-3-319-52669-0

Barkade, S. S., Bansod, P. G., Doss, V. R., & Mardikar, S. P. (2020). Development of Poly(aspartic-co-glutamic acid) Green Antiscalant for Calcium Carbonate Scale Inhibition. *Advanced Science, Engineering and Medicine*, *12*(2), 198–206. https://doi.org/10.1166/asem.2020.2488

Bednarz, S., Błaszczyk, A., Błazejewska, D., & Bogdał, D. (2015). Free-radical polymerization of itaconic acid in the presence of choline salts: Mechanism of persulfate decomposition. *Catalysis Today*, *257*(Part 2), 297–304. https://doi.org/10.1016/j.cattod.2014.07.021

Bednarz, S., Wesołowska-Piętak, A., Konefał, R., & Świergosz, T. (2018). Persulfate initiated free-radical polymerization of itaconic acid: Kinetics, end-groups and side products. *European Polymer Journal*, *106*, 63–71. https://doi.org/10.1016/j.eurpolymj.2018.07.010

Bello, O. (2017). *Calcium Carbonate Scale Deposition Kinetics on Stainless Steel Surfaces* (Issue January) [The University of Leeds]. https://etheses.whiterose.ac.uk/17647/1/Thesis_final_version.pdf

Bouchama, F., Van Aken, G. A., Autin, A. J. E., & Koper, G. J. M. (2003). On the

mechanism of catastrophic phase inversion in emulsions. *Colloids and Surfaces A: Physicochemical and Engineering Aspects*, *231*(1–3), 11–17. https://doi.org/10.1016/j.colsurfa.2003.08.011

Calcium and Water Hardness. (2011). LEO EnviroSci Inquiry. https://ei.lehigh.edu/envirosci/watershed/wq/wqbackground/calciumbg.html

Cao, M. (2008a). *Synthesis and Properties of poly(itaconic acid)*. University of New Hampshire Schola's Repository.

Cao, M. (2008b). *Synthesis and Properties of Poly(itaconic acid)* [University of New Hampshire, Durham]. https://scholars.unh.edu/cgi/viewcontent.cgi?article=1376&context=thesis

Cao, M. (2008c). *Synthesis and Properties of Poly (itaconic acid)*. https://scholars.unh.edu/cgi/viewcontent.cgi?article=1376&context=thesis

Chew, C. B., & Mat, R. (2015). The efficacy of calcium carbonate scale inhibition by commercial polymer scale inhibitors. *Chemical Engineering Transactions*, *45*(October 2015), 1471–1476. https://doi.org/10.3303/CET1545246

Choi, H., Park, J., & Lee, J. (2022). Sustainable Bio-Based Superabsorbent Polymer: Poly(itaconic acid) with Superior Swelling Properties. In *ACS Applied Polymer Materials* (Vol. 4, Issue 6). https://doi.org/10.1021/acsapm.2c00021

Cui, C., & Zhang, S. (2019). Synthesis, characterization and performance evaluation of an environmentally benign scale inhibitor IA/AMPS co-polymer. *New Journal of Chemistry*, *43*(24), 9472–9482. https://doi.org/10.1039/c9nj01355e

Cummings, S., Zhang, Y., Kazemi, N., Penlidis, A., & Dubé, M. A. (2016). Determination of reactivity ratios for the copolymerization of poly(acrylic acid-co-itaconic acid). *Journal of Applied Polymer Science*, *133*(40), 6–11. https://doi.org/10.1002/app.44014

Cunha da Cruz, J., Machado de Castro, A., & Camporese Sérvulo, E. F. (2018). World market and biotechnological production of itaconic acid. *3 Biotech*, *8*(3). https://doi.org/10.1007/s13205-018-1151-0

da Cruz, J. C., Camporese Sérvulo, E. F., & de Castro, A. M. (2017). Microbial Production of Itaconic Acid. In *Microbial Production of Food Ingredients and Additives* (Issue November). Elsevier Inc. https://doi.org/10.1016/b978-0-12-811520-6.00010-6

Dai, J., Ma, S., Wu, Y., Han, L., Zhang, L., Zhu, J., & Liu, X. (2015). Polyesters derived from itaconic acid for the properties and bio-based content enhancement of soybean oil-based thermosets. *Green Chemistry*, *17*(4), 2383–2392. https://doi.org/10.1039/c4gc02057j

Devasia, R., Reghunadhan Nair, C. P., & Ninan, K. N. (2003). Copolymerization of acrylonitrile with itaconic acid in dimethylformamide: Effect of triethylamine. *European Polymer Journal*, *39*(3), 537–544. https://doi.org/10.1016/S0014-3057(02)00275-6

Du, Q., Wang, Y., Li, A., & Yang, H. (2018). Scale-inhibition and flocculation dual-functionality of poly(acrylic acid) grafted starch. *Journal of Environmental Management*, *210*, 273–279. https://doi.org/10.1016/j.jenvman.2018.01.016

Duggirala, P. (2005). Formation of calcium carbonate scale and control strategies in continuous digesters. *CD Del II Coloquio Internacional Sobre Celulosa …*. http://www.eucalyptus.com.br/icep02/prassad_duggirala.pdf

Erbil, C., & Uyank, N. (2001). Interactions between poly(acrylamide)-poly(itaconic acid) and cerium(IV)- Nitrilotriacetic acid redox pair in the synthesis of acrylamide and itaconic acid homo- And copolymers. *Polymer International*, *50*(7), 792–795. https://doi.org/10.1002/pi.697

Ferreira, A. M., Vikulina, A. S., & Volodkin, D. (2020). CaCO3 crystals as versatile carriers for controlled delivery of antimicrobials. *Journal of Controlled Release*, *328*(July), 470–489. https://doi.org/10.1016/j.jconrel.2020.08.061

Filtration, C. (2022). *Acidity*. Cummins Filtration. Retrieved from https://www.cumminsfiltration.com/eme/acidity

Fink, J. (2015). Scale inhibitors. *Petroleum Engineer's Guide to Oil Field Chemicals and Fluids*, 255–278. https://doi.org/10.1016/b978-0-12-803734-8.00007-2

Frenkel, V. S., Pervov, A. G., Andrianov, A. P., & Golovesov, V. A. (2019). Investigation of antiscalant dosing influence on scaling process in reverse osmosis facilities and membrane surface adsorption. *Vestnik MGSU*, *6*, 722–733. https://doi.org/10.22227/1997-0935.2019.6.722-733

Goldberg, I., & Stefan Rokem, J. (2019). Organic and fatty acid production, microbial. *Encyclopedia of Microbiology*, 358–382. https://doi.org/10.1016/B978-0-12-809633-8.13083-3

Greenlee, L. F., Testa, F., Lawler, D. F., Freeman, B. D., & Moulin, P. (2010). The effect of antiscalant addition on calcium carbonate precipitation for a simplified synthetic brackish water reverse osmosis concentrate. *Water Research*, *44*(9), 2957–2969. https://doi.org/10.1016/j.watres.2010.02.024

Hoang, T. A. (2015). Mechanisms of Scale Formation and Inhibition. In P. Department of Chemical Engineering, Curtin University of Technology (Ed.), *Mineral Scales and Deposits: Scientific and Technological Approaches*. Elsevier B.V. https://doi.org/10.1016/B978-0-444-63228-9.00003-6

House, D. A. (1962). Kinetics and mechanism of oxidations by peroxydisulfate. *Chemical Reviews*, *62*(3), 185–203. https://doi.org/10.1021/cr60217a001

Huang, H., Yao, Q., Jiao, Q., Liu, B., & Chen, H. (2019). Polyepoxysuccinic acid with hyper-branched structure as an environmentally friendly scale inhibitor and its scale inhibition mechanism. *Journal of Saudi Chemical Society*, *23*(1), 61–74. https://doi.org/10.1016/j.jscs.2018.04.003

Jafar Mazumder, M. A. (2020). A review of green scale inhibitors: Process, types, mechanism and properties. *Coatings*, *10*(10), 1–29. https://doi.org/10.3390/coatings10100928

Jerome, K., Anne, W., Satoru, T., Katja, S., & Margret, A. (2022). 2-Phosphonobutane-1,2,4,-Tricarboxylic Acid (PBTC): pH-Dependent Behavior Studied by Means of Multinuclear NMR Spectroscopy. *Molecules*, *27*, 1–13. https://doi.org/10.1039/PC9928900003

Joy Bell, S. S., & Subhashini, S. (2018). Self-Assembled Chitosan-g-Poly(itaconic acid) Nanopparticle:A Potential Drug Carrier for Docetaxel. *Asian Journal of Chemistry*, *30*(18), 1470–1475.

Kakurkin, N. P., Malashenko, A. A., Pudova, N. E., & Perunova, E. Y. (2019). Investigation of calcium carbonate precipitation in the presence of scale inhibitors. *IOP Conference Series: Earth and Environmental Science*, *288*(1). https://doi.org/10.1088/1755-1315/288/1/012010

Kiran D. Dhawale, Nitin M. Thorat, L. R. P. (2018). Self-Assembled Chitosan-g-Poly(itaconic acid) Nanoparticles: A Potential Drug Carrier for Docetaxel. *Asian Journal of Chemistry*, *30*(18), 2424–2430. https://doi.org/10.14233/ajchem.2017.20553

Kirimura, K., Honda, Y., & Hattori, T. (2011). Gluconic and Itaconic Acids. In *Comprehensive Biotechnology, Second Edition* (Second Edi, Vol. 3). Elsevier B.V. https://doi.org/10.1016/B978-0-08-088504-9.00175-6

Korbag, I., & Mohamed Saleh, S. (2016). Studies on the formation of intermolecular interactions and structural characterization of polyvinyl alcohol/lignin film. *International Journal of Environmental Studies*, *73*(2), 226–235. https://doi.org/10.1080/00207233.2016.1143700

Krull, S., Hevekerl, A., Kuenz, A., & Prüße, U. (2017). Process development of itaconic acid production by a natural wild type strain of Aspergillus terreus to reach industrially relevant final titers. *Applied Microbiology and Biotechnology*, *101*(10), 4063–4072. https://doi.org/10.1007/s00253-017-8192-x

Kulal, P., & Badalamoole, V. (2021). Evaluation of gum ghatti-g-poly(itaconic acid) magnetite nanocomposite as an adsorbent material for water purification. *International Journal of Biological Macromolecules*, *193*(PB), 2232–2242. https://doi.org/10.1016/j.ijbiomac.2021.11.055

Kumar, A., Li, S., Cheng, C. M., & Lee, D. (2015). Recent Developments in Phase Inversion Emulsification. *Industrial and Engineering Chemistry Research*, *54*(34), 8375–8396. https://doi.org/10.1021/acs.iecr.5b01122

Kumar, M., Bishnoi, R. S., Shukla, A. K., & Jain, C. P. (2019). Techniques for formulation of nanoemulsion drug delivery system: A review. *Preventive Nutrition and Food Science*, *24*(3), 225–234. https://doi.org/10.3746/pnf.2019.24.3.225

Li, H., Liu, W., & Qi, X. (2007). Evaluation of a novel CaSO4 scale inhibitor for a reverse osmosis system. *Desalination*, *214*(1–3), 193–199. https://doi.org/10.1016/j.desal.2006.10.023

Li, H. Y., Ma, W., Wang, L., Liu, R., Wei, L. Sen, & Wang, Q. (2006). Inhibition of calcium and magnesium-containing scale by a new antiscalant polymer in laboratory tests and a field trial. *Desalination*, *196*(1–3), 237–247. https://doi.org/10.1016/j.desal.2005.11.024

Li, J., Liu, D., Jiang, H., Wang, J., Jing, X., Chen, R., Zhu, W., Han, S., Li, W., & Wei, H. (2016). Effects of polyacrylic acid additive on barium sulfate particle morphology. *Materials Chemistry and Physics*, *175*, 180–187.

https://doi.org/10.1016/j.matchemphys.2016.03.015

Li, X., Gao, B., Yue, Q., Ma, D., Rong, H., Zhao, P., & Teng, P. (2015). Effect of six kinds of scale inhibitors on calcium carbonate precipitation in high salinity wastewater at high temperatures. *Journal of Environmental Sciences (China)*, *29*, 124–130. https://doi.org/10.1016/j.jes.2014.09.027

Liu, W., Sun, D., Li, C., Liu, Q., & Xu, J. (2006). Formation and stability of paraffin oil-in-water nano-emulsions prepared by the emulsion inversion point method. *Journal of Colloid and Interface Science*, *303*(2), 557–563. https://doi.org/10.1016/j.jcis.2006.07.055

Liu, Y., Zhou, Y., Yao, Q., Huang, J., Liu, G., Wang, H., Cao, K., Chen, Y., Bu, Y., Wu, W., & Sun, W. (2014). Double-hydrophilic polyether antiscalant used as a crystal growth modifier of calcium scales in cooling-water systems. *Journal of Applied Polymer Science*, *131*(2), 1–12. https://doi.org/10.1002/app.39792

Liu, Z., Yan, M., Liu, Z., & Li, N. (2019). Synthesis and properties of the IA/AMPS copolymer. *IOP Conference Series: Earth and Environmental Science*, *330*(4). https://doi.org/10.1088/1755-1315/330/4/042049

Luo, H., Chen, D., Yang, X., Zhao, X., Feng, H., Li, M., & Wang, J. (2015). Synthesis and performance of a polymeric scale inhibitor for oilfield application. *Journal of Petroleum Exploration and Production Technology*, *5*(2), 177–187. https://doi.org/10.1007/s13202-014-0123-0

Malik, S., Mondal, M. H., Ghosh, A., De, S., Mahali, K., Bhattacharyya, S. S., & Saha, B. (2016). Combination of Sodium Dodecylsulfate and 2,2′-Bipyridine for Hundred Fold Rate Enhancement of Chromium(VI) Oxidation of Malonic Acid at Room Temperature: A Greener Approach. *Journal of Solution Chemistry*, *45*(7), 1043–1060. https://doi.org/10.1007/s10953-016-0494-6

Mengmeng, Y., Hou, C., Ying, L., Hengli, C., Wenying, Z., Xianqiang, C., & Dongmei, L. (2008). Porous Acrylonitrile/Itaconic Acid Copolymers Prepared by Suspended Emulsion Polymerization. *Journal of Applied Polymer Science*, *111*, 2762–2768. https://doi.org/10.1002/app.29339

Mohammadinezhad, A., Marandi, G. B., Farsadrooh, M., & Javadian, H. (2018). Synthesis of poly(acrylamide-co-itaconic acid)/MWCNTs superabsorbent hydrogel nanocomposite by ultrasound-assisted technique: Swelling behavior

and Pb (II) adsorption capacity. *Ultrasonics Sonochemistry*, *49*(Ii), 1–12. https://doi.org/10.1016/j.ultsonch.2017.12.028

Mohanty, S., Das, B., & Dhara, S. (2013). Poly(maleic acid) - A novel dispersant for aqueous alumina slurry. *Journal of Asian Ceramic Societies*, *1*(2), 184–190. https://doi.org/10.1016/j.jascer.2013.05.005

Naghash, H. J., Mallakpour, S., & Kayhan, N. (2005). Synthesis and characterization of silicone modified acrylic resin and its uses in the emulsion paints. *Iranian Polymer Journal (English Edition)*, *14*(3), 211–222.

Okada, H., Zhao, C., Mizuta, Y., Yoshino, K., & Sugimoto, R. (2021). Emulsion Graft Polymerization of Methyl Methacrylate onto Cellulose Nanofibers. *Green and Sustainable Chemistry*, *11*(01), 9–22. https://doi.org/10.4236/gsc.2021.111002

Oshchepkov, M. S., Pervov, A. G., Golovesov, V. A., Rudakova, G. Y., Kamagurov, S. D., Tkachenko, S. V., Andrianov, A. P., & Popov, K. I. (2019). Use of a Fluorescent Antiscalant to Investigate Scaling of Reverse Osmosis Membranes. *Membranes and Membrane Technologies*, *1*(4), 254–266. https://doi.org/10.1134/S2517751619040061

Popov, K., Rudakova, G., Larchenko, V., Tusheva, M., Kamagurov, S., Dikareva, J., & Kovaleva, N. (2016). A Comparative Performance Evaluation of Some Novel "Green" and Traditional Antiscalants in Calcium Sulfate Scaling. *Advances in Materials Science and Engineering*, *2016*. https://doi.org/10.1155/2016/7635329

Preziosi, V., Perazzo, A., Caserta, S., Tomaiuolo, G., & Guido, S. (2013). Phase inversion emulsification. *Chemical Engineering Transactions*, *32*, 1585–1590. https://doi.org/10.33032/CET1332265

Scientific, T. F. (2022). *No TItaconic acid, 99+%, Thermo Scientific™itle*. Thermo Fisher Scientific. Retrieved from https://www.fishersci.se/shop/products/itaconic-acid-99-thermo-scientific-4/10549040

Sheng, K., Ge, H., Huang, X., Zhang, Y., Song, Y., Ge, F., Zhao, Y., & Meng, X. (2020). Formation and Inhibition of Calcium Carbonate Crystals under Cathodic Polarization Conditions. *Crystals*, *10*(4). https://doi.org/10.3390/cryst10040275

Shi, W., Xu, W., Cang, H., Yan, X., Shao, R., Zhang, Y., & Xia, M. (2017). Design

and synthesis of biodegradable antiscalant based on MD simulation of antiscale mechanism: A case of itaconic acid-epoxysuccinate copolymer. *Computational Materials Science*, *136*, 118–125. https://doi.org/10.1016/j.commatsci.2017.04.035

Singh, Y. B., & Ng, K. C. (2019). Elucidation of dual-mode inhibition mechanism of a typical polymer-based antiscalant on Red seawater for thermal desalination at higher temperatures and higher concentration factors. *Journal of Petroleum Science and Engineering*, *183*(July), 106380. https://doi.org/10.1016/j.petrol.2019.106380

Sirviö, J. A., Kantola, A. M., Komulainen, S., & Filonenko, S. (2021). Aqueous modification of chitosan with itaconic acid to produce strong oxygen barrier film. *Biomacromolecules*, *22*(5), 2119–2128. https://doi.org/10.1021/acs.biomac.1c00216

Sriariyanun, M., Heitz, J. H., Yasurin, P., Asavasanti, S., & Tantayotai, P. (2019). Itaconic acid: A promising and sustainable platform chemical? *Applied Science and Engineering Progress*, *12*(2), 75–82. https://doi.org/10.14416/j.asep.2019.05.002

Stanley Walter, W., & James William, M. (1983). Polyitaconic acid Threshold scale inhibitor. *European Patent Application*, *1645*, 1–76. https://patentimages.storage.googleapis.com/ff/12/8e/eda82757d69067/EP0090574A1.pdf

Suo, G., Xie, L., Xu, S., Feng, L., Dong, T., & Shao, X. (2018). Study on inhibitors' performance under the condition of high concentration ratio in MED system. *Desalination*, *437*(November 2017), 100–107. https://doi.org/10.1016/j.desal.2018.02.019

Tang, M., Li, J., Ye, Z., Kou, Z., & Fu, L. (2017). A Novel Eco-Friendly Scale and Corrosion Inhibitor Modified by β-Cyclodextrin. *Australian Journal of Chemistry*, *70*(8), 933–942. https://doi.org/10.1071/CH16720

Thananukul, K., Petchsuk, A., Supmak, W., Chaiyasat, P., Chaiyasat, A., & Opaprakasit, P. (2018). Preparation of Crosslinked Poly (lactic acid-co- glycidyl methacrylate) Microspheres by Phase Inversion Emulsification. *Chiang Mai Journal of Science*, *45*(5), 2048–2058.

https://www.thaiscience.info/Journals/Article/CMJS/10990171.pdf

van Berkel, K. Y., Russell, G. T., & Gilbert, R. G. (2006). The dissociation rate coefficient of persulfate in emulsion polymerization systems. *Polymer*, *47*(13), 4667–4675. https://doi.org/10.1016/j.polymer.2006.04.048

Wierckx, N., Agrimi, G., Lübeck, P. S., Steiger, M. G., Mira, N. P., & Punt, P. J. (2020). Metabolic specialization in itaconic acid production: a tale of two fungi. *Current Opinion in Biotechnology*, *62*, 153–159. https://doi.org/10.1016/j.copbio.2019.09.014

World Health Organisation. (2007). pH in drinking-water. In *Guidelines for drinking water quality* (Vol. 2, Issue 2). http://www.who.int/water_sanitation_health/dwq/chemicals/ph_revised_2007_clean_version.pdf

Xiao, Y., Ren, D., Li, H., Wang, Z., Zhai, J., Xie, J., Zhang, S., Zhang, X., & Chen, W. (2022). Study on synthesis and property of multi-copolymer scale inhibitor. *Journal of Polymer Research*, *29*(11). https://doi.org/10.1007/s10965-022-03337-3

Yang, L., Yang, W., Xu, B., Yin, X., Chen, Y., Liu, Y., Ji, Y., & Huan, Y. (2017). Synthesis and scale inhibition performance of a novel environmental friendly and hydrophilic terpolymer inhibitor. *Desalination*, *416*(May), 166–174. https://doi.org/10.1016/j.desal.2017.05.010

Zhang, S., Qu, H., Yang, Z., Fu, C. e., Tian, Z., & Yang, W. (2017). Scale inhibition performance and mechanism of sulfamic/amino acids modified polyaspartic acid against calcium sulfate. *Desalination*, *419*(May), 152–159. https://doi.org/10.1016/j.desal.2017.06.016

Zhao, L., Zhou, Y., Yao, Q., Wang, Y., Ge, S., & Liu, X. (2021). Calcium Scale Inhibition of Stimulated Oilfield Produced Water Using Polyaspartic Acid/Aminomethanesulfonic Acid. *ChemistrySelect*, *6*(15), 3692–3701. https://doi.org/10.1002/slct.202100853

Zhou, M., Gu, Y., Yi, R., & Han, H. (2020). Synthesis and property study of ter-copolymer P(MA-AMPS-HPA) scale inhibitor. *Journal of Polymer Research*, *27*(10). https://doi.org/10.1007/s10965-020-02270-7

APPENDICES

APPENDIX A

MOLECULAR WEIGHT OF PIA FROM GPC

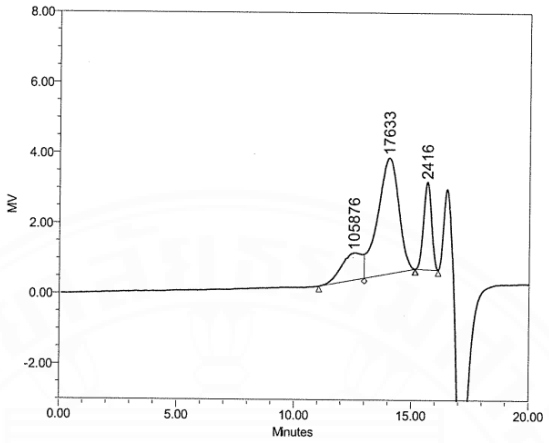

	Mn (Daltons)	Mw (Daltons)	MP (Daltons)	Mz (Daltons)	Mz+1 (Daltons)	Polydispersity	% Area	Area
1	115994	142767	105876	181624	231197	1.2308	15.56	48328
2	17006	21848	17633	28141	35056	1.2848	65.81	204419
3	2366	2447	2416	2532	2618	1.0344	18.63	57860

Figure A.1 Molecular weight of EP-N30

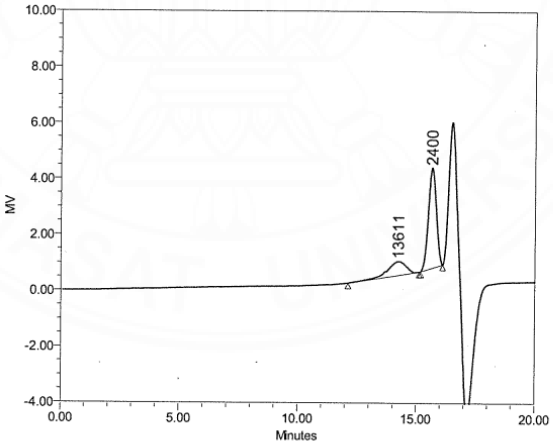

	Mn (Daltons)	Mw (Daltons)	MP (Daltons)	Mz (Daltons)	Mz+1 (Daltons)	Polydispersity	% Area	Area
1	14501	19216	13611	31215	58600	1.3252	24.82	27409
2	2367	2447	2400	2531	2618	1.0341	75.18	83020

Figure A.2 Molecular weight of PI-N30

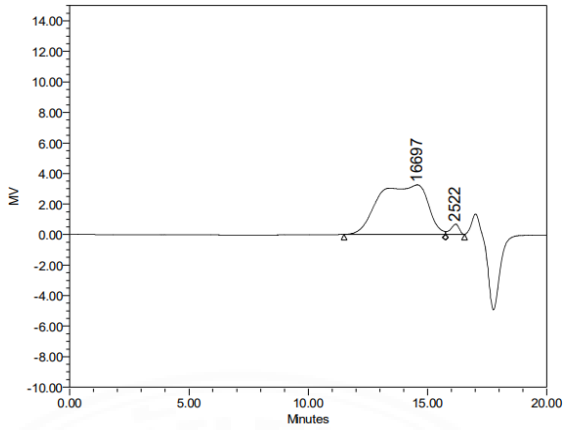

	Mn (Daltons)	Mw (Daltons)	MP (Daltons)	Mz (Daltons)	Mz+1 (Daltons)	Polydispersity	% Area	Area
1	24486	56454	16697	112981	175822	2.3056	96.61	466953
2	2637	2736	2522	2845	2960	1.0376	3.39	16410

Figure A.3 Molecular weight of FR-PH4

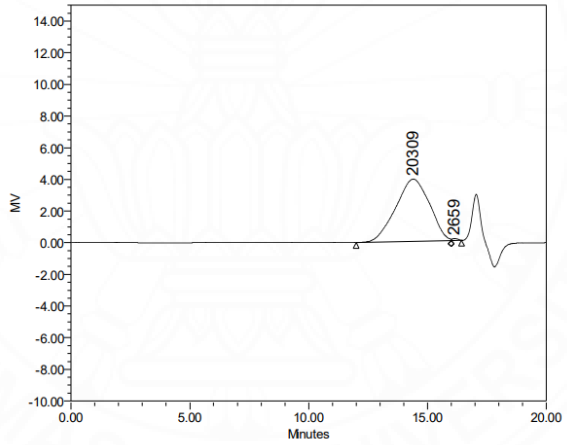

	Mn (Daltons)	Mw (Daltons)	MP (Daltons)	Mz (Daltons)	Mz+1 (Daltons)	Polydispersity	% Area	Area
1	16332	28427	20309	49130	76241	1.7406	99.45	389368
2	2559	2594	2659	2629	2663	1.0139	0.55	2156

Figure A.4 Molecular weight of FR-PH5

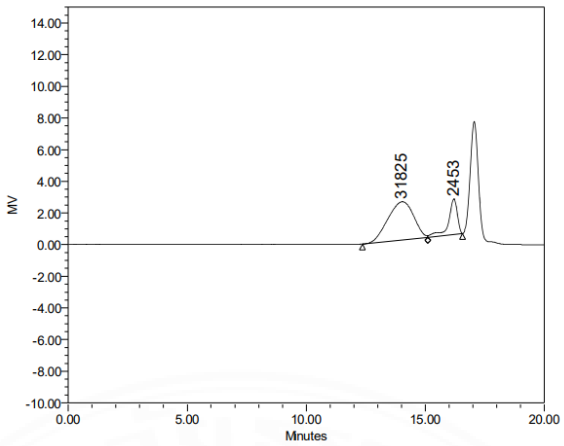

	Mn (Daltons)	Mw (Daltons)	MP (Daltons)	Mz (Daltons)	Mz+1 (Daltons)	Polydispersity	% Area	Area
1	29933	40159	31825	53763	69189	1.3416	75.65	181650
2	2693	3026	2453	3611	4497	1.1235	24.35	58459

Figure A.5 Molecular weight of FR-A5

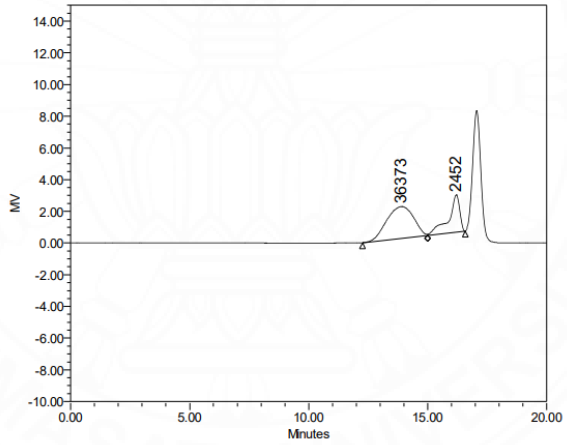

	Mn (Daltons)	Mw (Daltons)	MP (Daltons)	Mz (Daltons)	Mz+1 (Daltons)	Polydispersity	% Area	Area
1	34270	46402	36373	62134	79365	1.3540	66.93	158347
2	2963	3477	2452	4242	5166	1.1733	33.07	78234

Figure A.6 Molecular weight of FR-A8

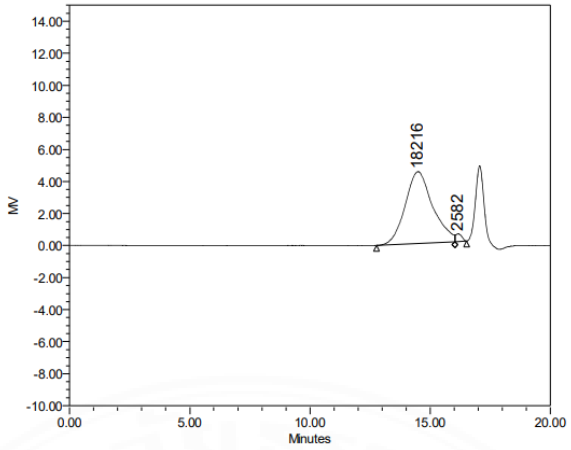

	Mn (Daltons)	Mw (Daltons)	MP (Daltons)	Mz (Daltons)	Mz+1 (Daltons)	Polydispersity	% Area	Area
1	13209	20087	18216	28759	38862	1.5207	97.66	355980
2	2457	2494	2582	2530	2564	1.0151	2.34	8521

Figure A.7 Molecular weight of FR-A14

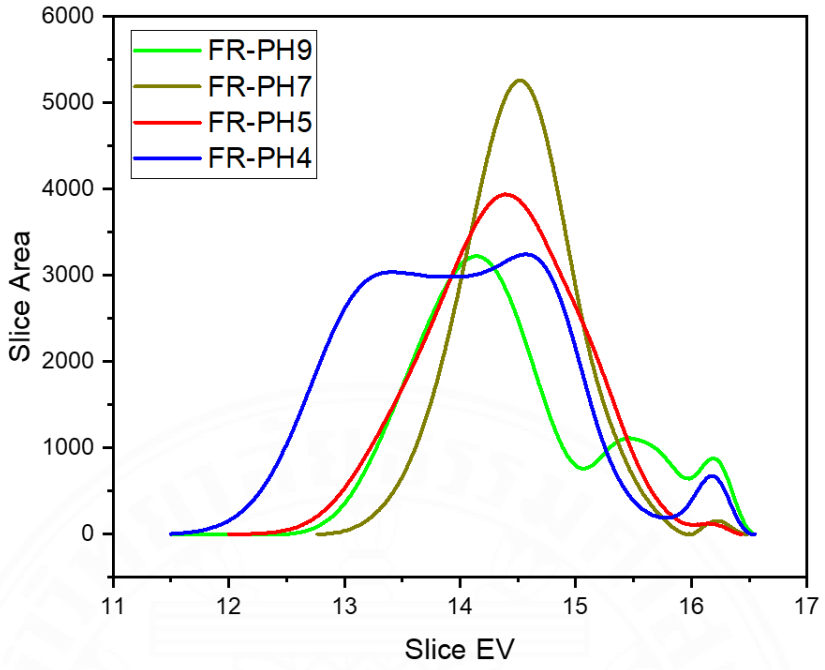

Figure A.8 GPC molecular weight distribution curves of FR-PH4, FR-PH5, FR-PH7, and FR-PH9

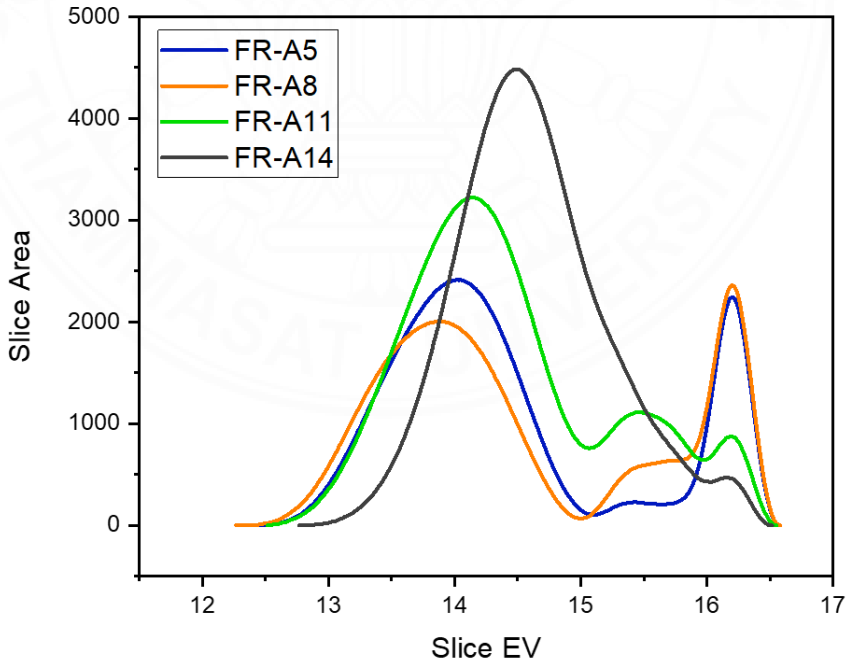

Figure A.9 GPC molecular weight distribution curves of FR-A5, FR-A8, FR-A11, and FR-A14.

APPENDIX B

FTIR ANALYSIS AND STANDARD CALIBRATION CURVE OF $[CA^{2+}]$ FOR ICP-OES

Table B.1 The wavenumber of calcium carboxylate and sodium carboxylate

Sample	V_{as} (COO^-) (cm^{-1})	V_s (COO^-) (cm^{-1})	ΔV_{Ca} (COO^-) (cm^{-1})	ΔV_{Na} (COO^-) (cm^{-1})
FR-PH4	1557	1398	159	163
FR-PH5	1552	1390	162	170
FR-PH7	1550	1386	164	162
FR-PH9	1550	1385	165	163
FR-A5	1552	1386	166	164
FR-A8	1549	1385	164	162
FR-A14	1549	1387	162	166

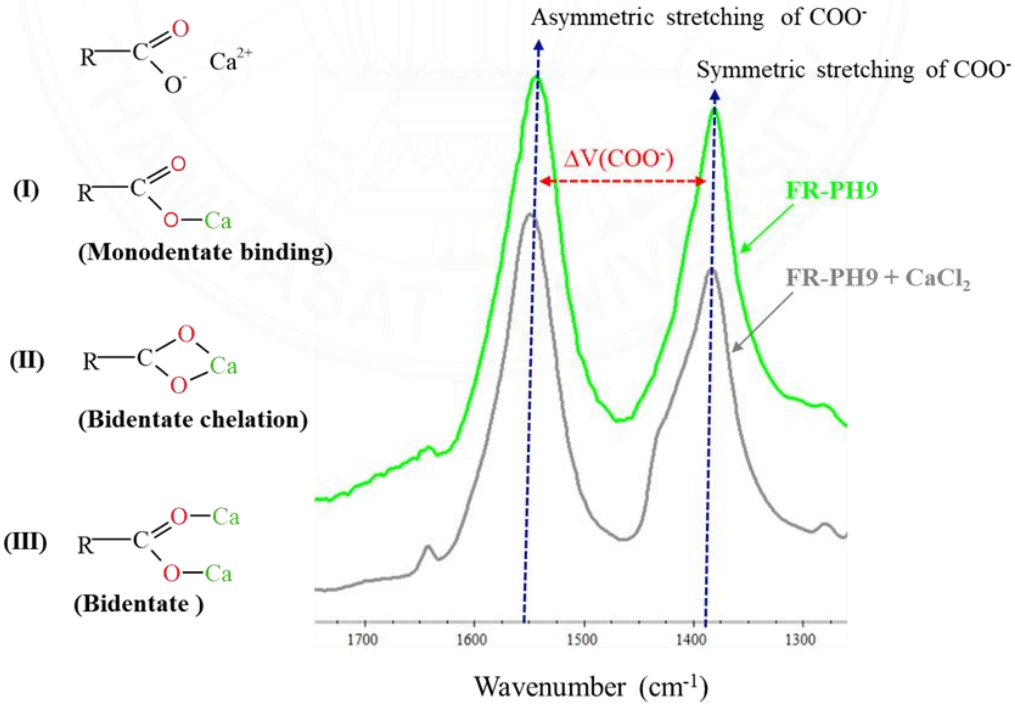

Figure B.1 FTIR spectra of FR-PH9 with $CaCl_2$ and propose their carboxylate binding modes.

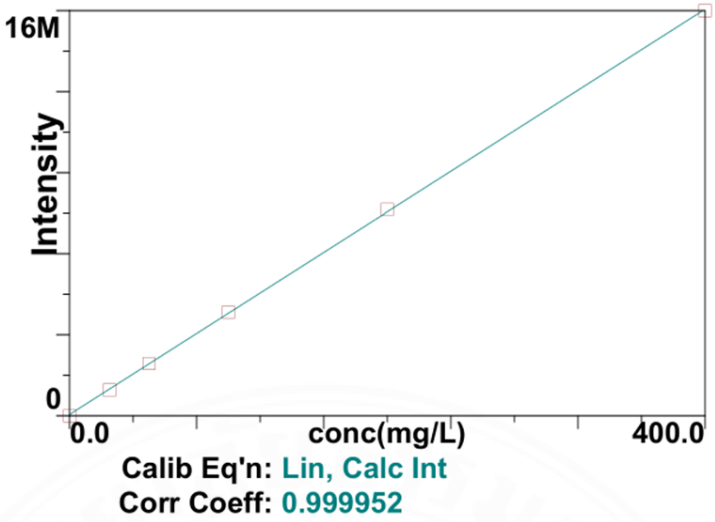

Figure B.2 Standard calibration curve of [Ca^{2+}] for ICP-OES measurement.

BIOGRAPHY

Name	Chakriya Kong
Education	2021: Bachelor of Engineering (Chemical and Food Engineering) Institute of Technology of Cambodia (ITC)
Publication	

Chakriya, K., Atitsa, P., & Pakorn, O. (2023). Bio-based antiscalant derived from poly(itaconic acid). *Proceedings of the 4th Materials Research Society of Thailand International Conference (MRS-Thailand 2023), 28 February - 4 March 2023, Ubon Ratchathani, Thailand*. (Accepted on 07/07/2023).